

Review

# Atropselective Organocatalytic Synthesis of Chiral Compounds Containing Nitrogen along the Axis of Chirality

Ana Maria Faisca Phillips <sup>1,\*</sup>  and Armando J. L. Pombeiro <sup>1,2</sup> 

<sup>1</sup> Coordination Chemistry and Catalysis Group, Centro de Química Estrutural, Institute of Molecular Sciences, Instituto Superior Técnico, Universidade de Lisboa, Av. Rovisco Pais 1, 1049-001 Lisboa, Portugal; pombeiro@tecnico.ulisboa.pt

<sup>2</sup> Research Institute of Chemistry, Peoples' Friendship University of Russia (RUDN University), 117198 Moscow, Russia

\* Correspondence: anafaiscaphillips@tecnico.ulisboa.pt

**Abstract:** Atropisomers, i.e., stereoisomers that are distinct because their free rotation about a single bond is hindered by steric interactions between nearby bulky groups or by electrostatics, may interact with their surroundings in different ways, and may also exhibit different properties. They may be found as natural products, as pharmaceutical or agricultural active ingredients, as chiral ligands and organocatalysts, and in functional materials. Our ability to synthesize them stereoselectively and in a sustainable way, using achiral materials and simply with the aid of an organocatalyst and mild conditions, has become a hot topic in research. This review provides an overview of recent achievements in the synthesis of atropisomers containing C-N and N-N axes of chirality.

**Keywords:** axial chirality; atropisomer; rotational energy barrier; stereoisomer; amination; C-H activation; annulation; desymmetrization; N-H functionalization



**Citation:** Faisca Phillips, A.M.; Pombeiro, A.J.L. Atropselective Organocatalytic Synthesis of Chiral Compounds Containing Nitrogen along the Axis of Chirality. *Symmetry* **2023**, *15*, 1261. <https://doi.org/10.3390/sym15061261>

Academic Editors: Fabrizio Vetica and Jesús F. Arteaga

Received: 17 May 2023

Revised: 7 June 2023

Accepted: 12 June 2023

Published: 15 June 2023



**Copyright:** © 2023 by the authors. Licensee MDPI, Basel, Switzerland. This article is an open access article distributed under the terms and conditions of the Creative Commons Attribution (CC BY) license (<https://creativecommons.org/licenses/by/4.0/>).

## 1. Introduction

Axially chiral compounds are those that may be differentiated into stereoisomers due to a nonplanar arrangement of four groups in pairs about a chirality axis, according to IUPAC rules [1]. Included in this group are atropisomers, which are non-superimposable stereoisomers because their rotation about a single bond is restricted due to clashes in the steric bulk of large substituents in close proximity. The restriction in rotation may also arise from dipole–dipole interactions or from other electrostatic interactions [2].

Whereas stereoisomers differing in point chirality can only be converted into one another by a bond-breaking, bond-making process, the interconversion of atropisomers is a time- and temperature-dependent dynamic process, which requires only rotation around a single bond, the axis of chirality. Hence, the rotational energy barrier ( $\Delta E_{\text{rot}}$ ) and the interconversion rate between an atropisomeric pair are key parameters to consider when studying or synthesizing these compounds. To be observed, or even isolated when possible, they have to interconvert slowly, with a half-life of  $>1000$  s [3].

It is common practice nowadays to divide atropisomers into three classes according to the energy required for the interconversion between the two forms, or their half-life of racemization at 37 °C, a classification that was proposed by LaPlante and co-workers in 2011 [4]. Class 1 atropisomers include those that equilibrate rapidly ( $t_{1/2}$  less than minutes) and have rotational energy barriers of  $< \sim 20$  kcal mol<sup>-1</sup>; Class 2 atropisomers have a moderate rate of equilibration ( $t_{1/2}$  from hours to days) in solution at rt. This applies to atropisomers with barriers to torsion rotation of  $\Delta E_{\text{rot}} \approx 20\text{--}30$  kcal mol<sup>-1</sup>. Class 3 atropisomers have very slow equilibration ( $t_{1/2}$  in years,  $\Delta E_{\text{rot}} \gg \sim 30$  kcal mol<sup>-1</sup>), i.e., there is practically no interconversion. Substances included in this class are very similar to compounds with classical stereocenter-based chirality. They exist as single enantiomers if

there is one axis of chirality, and as diastereoisomers if there is more than one axis or center of chirality in the molecule.

There are many examples of atropisomerism in nature as natural products, as well as in pharmaceutical active ingredients (APIs) and agricultural products, in chiral ligands and organocatalysts, and in functional materials, including liquid crystals, chiroptical switches, coolants and lubricants, and even molecular rotors [4–7]. Some are shown in Figure 1. In chemistry and more particularly in asymmetric synthesis, many advances have been made due to the discovery of axially chiral ligands such as BINAP [8], BINOL [9], BINAM [10], and lately, of axially chiral phosphoric acid organocatalysts [11]. In recent years, atropisomers have also evolved from the classical structures consisting of identical bi(hetero)aryl skeletons only, such as the C<sub>2</sub>-symmetric binaphthyl-based catalysts referred to above, to scaffolds with a chirality axis joining two different rings, and even to those incorporating only one ring structure [12].

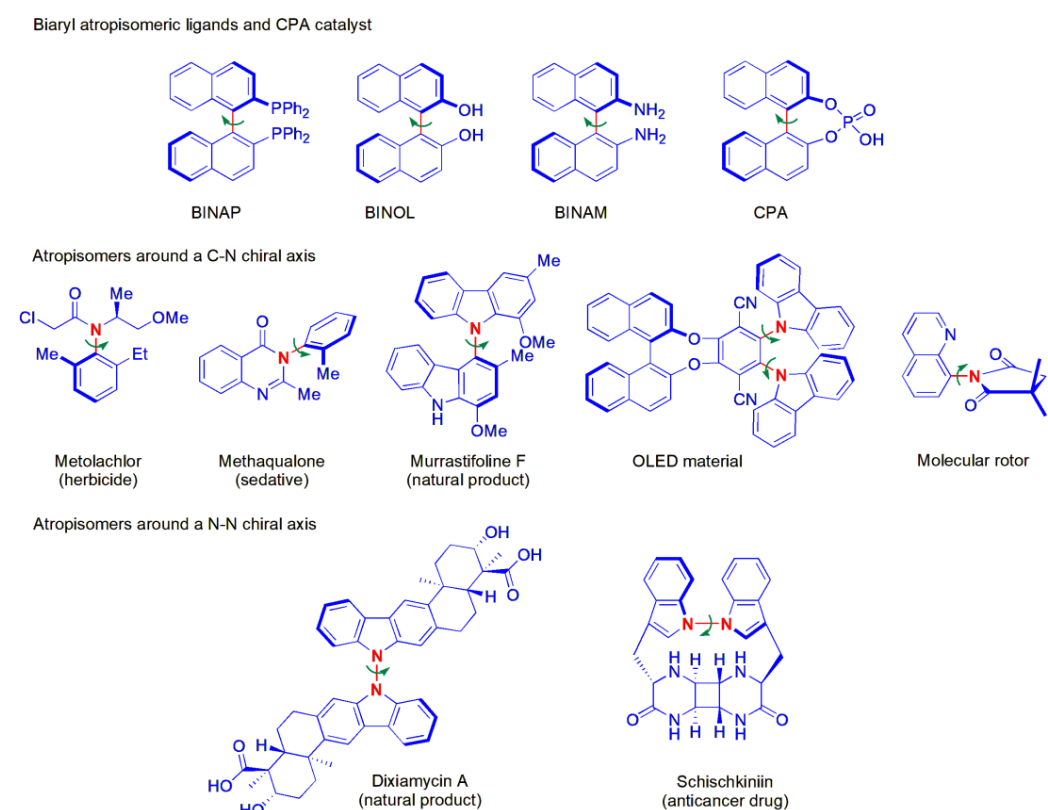


**Figure 1.** C-C, C-N and N-N atropisomers applied as chiral ligands, organocatalysts, pharmaceuticals, natural products, molecular rotors and host materials for OLEDs.

In medicinal chemistry, the need to identify atropisomerism has been long recognized to be of great importance in drug discovery, since as it happens with other types of stereoisomers; atropisomers may display quite different properties, such as in vitro inhibition, crystallization, in vivo racemization rates, and absorption, distribution, metabolism, excretion, and toxicity properties [13]. Atropisomerism used to be looked at as a “lurking menace”, which could not only be present unknowingly, but could also increase the cost of pharmaceutical research and development [14]. For example, there could be a need to modify parts of the structure of a drug candidate, in order to convert it from an unstable class 2 atropisomer, whose stereochemical integrity could be compromised during production or administration to patients, into a stable class 3 drug [14,15].

As new methods to obtain atropisomers are being developed, e.g., catalytic enantioselective synthesis [2,16], as well as ways to analyze the, e.g., variable temperature NMR for atropisomer mixtures, determination of rotational energy barriers ( $\Delta E_{rot}$ ) by density func-

tional theory (DFT) calculations and quantum mechanical calculations, which give a good estimate of the half-life for interconversion of the two forms, atropisomers, are being looked at more favorably [14]. Experimental methods including segmented flow technologies are also used to investigate the kinetics of interconversion [2]. The large number of reviews published in recent years show the growing attention that this area is receiving [2,12–18], including in the development of asymmetric methods of synthesis [19–31].

Atropisomerism in N-N bond-containing substances has been less explored. Although factors such as the short bond length, a more crowded axis, and the repulsion of the lone pairs on the two nitrogen atoms are favorable, the barrier to rotation is low, since the two N-containing planes can become deplanarized upon rotation, making it difficult to obtain these stereoisomers [32]. However, molecular interactions causing an energy barrier to rotation of  $>23 \text{ kcal mol}^{-1}$  can give rise to class 2 atropisomers [3,4] and this value can be obtained with H-bonding, ionic interactions, and  $\pi$ -stacking [3], which suggests that atropselective syntheses may be possible. These syntheses were indeed achieved for the first time by Houk, Lu, and co-workers in 2021. Examples of atropisomerism due to restricted rotation around a N-N bond have been found in nature, wherein it was discovered that the natural product dixiamycin could be isolated as a pair of atropisomers, A and B, with different activities against *Staph. aureus* and *B. thuringiensis* in 2012 [33]. Several new examples of the atropselective synthesis of different N-N axially chiral compounds have been recently reported.

In this survey, the literature related to organocatalytic enantioselective methods developed to produce atropisomers containing C-N and N-N axes of chirality is reviewed. The texts are divided firstly into methods for the synthesis of these two types of compounds, and subsequently into the type of general synthetic strategy used, as shown in Figure 2, for C-N axially chiral compounds: C-H amination, N-H functionalization, C-H functionalization, desymmetrization and atropselective annulation.

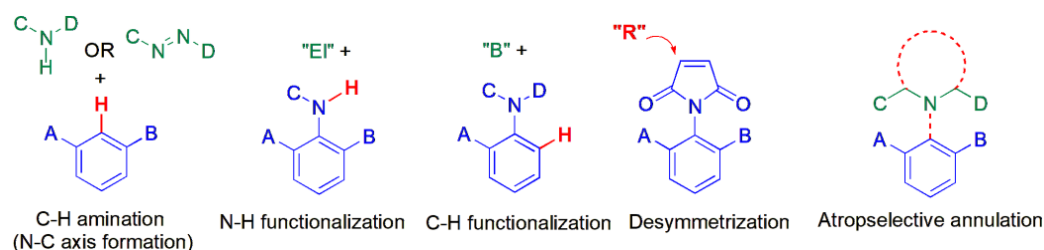


**Figure 2.** Strategies for the synthesis of C-N axially chiral compounds.

## 2. Atropisomers Containing a C-N Chirality Axis

### 2.1. C-H Amination

Non-biaryl atropisomers synthesized from 2-naphthol by means of asymmetric organocatalysis were described for the first time by Bella, Jørgensen and co-workers in 2006 [34]. The rotation along the chiral axis in these substances can be hindered by substituents in the *peri* position. Until then, the syntheses reported involved chiral resolution to obtain pure racemates [35], with one exception being an account of enantioselective synthesis utilizing a metal-catalyzed approach [36]. The amination of a series of 8-amino-2-naphthols (**1**) with di-*tert*-butyl azodicarboxylate (**2a**) in combination with dihydrocupreidine (**C1**) as a catalyst provided products (**3**) in high yields and good ees (Figure 3). The ee of **3a** ( $R^1 = \text{NH}_2$ ;  $R^2 = R^3 = \text{H}$ ) did not change much when the compound was kept at  $-20 \text{ }^\circ\text{C}$ , and at the room temperature, the ee dropped only 3% in 10 days. In an attempt to obtain more stereoselective catalysts, the group performed the same asymmetric Friedel–Crafts amination reaction of the cinchona alkaloid catalysts themselves, and subsequently used them, after chromatographic separation of the two diastereoisomers obtained, as catalysts to perform the reactions shown in Figure 3. Substantial enhancements in ee were obtained, e.g., with **C2**, compounds **3** were obtained with 87–98% ee.

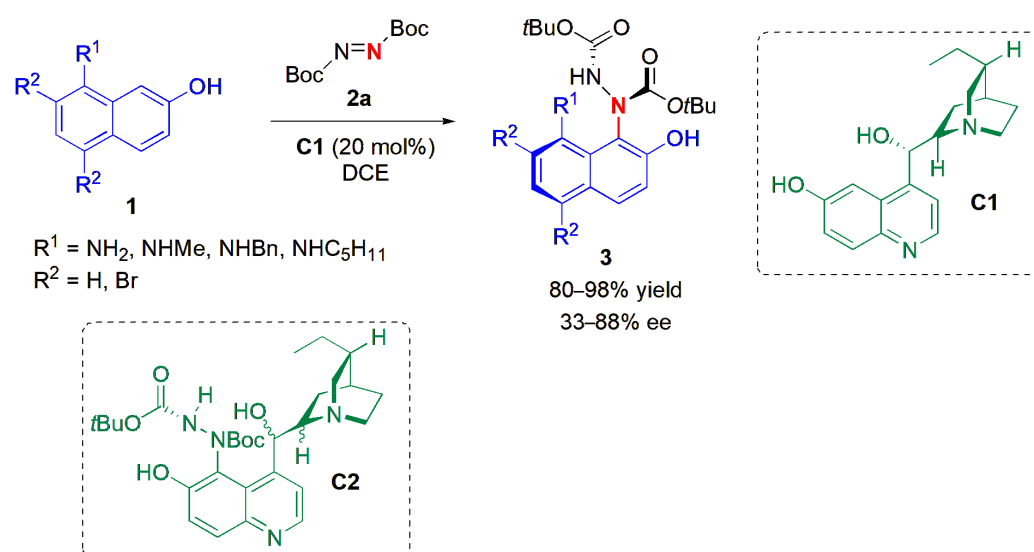


**Figure 3.** Asymmetric organocatalytic Friedel–Crafts amination of 2-naphthols for the synthesis of non-biaryl atropisomers [34].

In 2019, Bai, Zhang and co-workers described the synthesis of novel nonbiaryl C–N atropisomers, naphthalene-1,2-diamines **6**, obtained from *N*-aryl-2-naphthylamines **4** with azodicarboxylates **5** as amino sources (Figure 4) [37]. Until then, chiral nonbiaryl C–N atropisomers of 2-naphthylamine derivatives had not yet been discovered. A chiral phosphoric acid catalyst, **C3**, was found to promote the amination reaction, and a range of products could be obtained in high yields and ee values, provided a di-*tert*-butyl azodicarboxylate was used. With other dicarboxylates, the ees were substantially lower. Interestingly, when  $R^2 = p\text{-CN}$ , or if the substrate contained a *peri*  $\text{NH}_2$  substituent, no product was obtained at all. It was assumed that the stereoselectivity could be controlled by concerted  $\pi$ – $\pi$  interactions and dual hydrogen bonding between the chiral phosphoric acid catalyst and the two reactant molecules, as shown in A. Half-lives of racemization (in *n*-hexane at 25 °C) were measured to verify the stereo-stability of the products. The ee of **6a** in the solid state (90.10% ee) remained 90.04% ee after 90 h at  $-18$  °C. Presumably, H-bonding interactions help to stabilize the products.

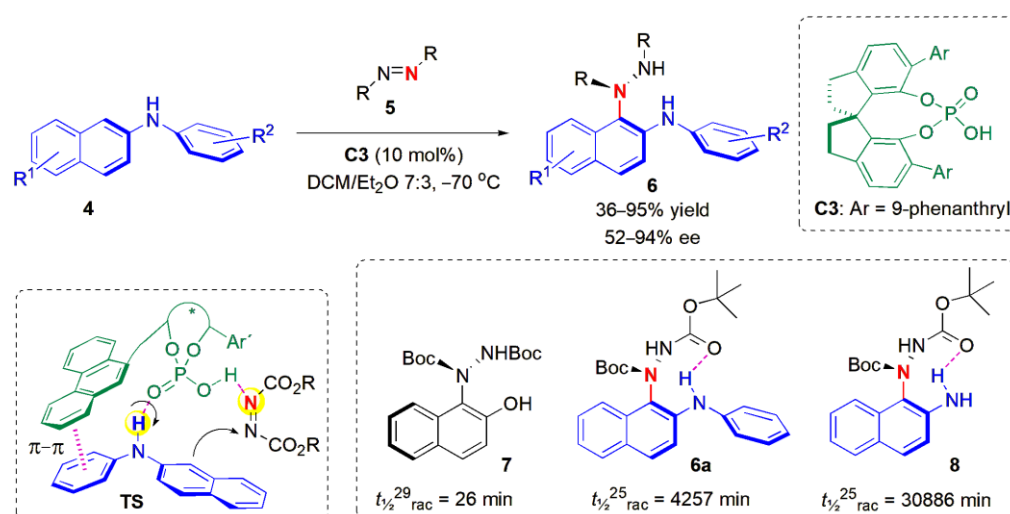


**Figure 4.** Atropselective synthesis of nonbiaryl naphthalene-1,2-diamine N–C atropisomers [37].

The direct aminations of 1,3-benzenediamines **9** with azodicarboxylates **5** have also been enabled by atropselective synthesis with chiral phosphoric acid catalysis, i.e., with (*S*)-**C4** (Figure 5a) [38]. By varying the nature of the N-substituents, benzene-substituents,

and azodicarboxylates, a range of C-N atropisomers **10** with high configurational stability were produced, with high yields and ees.

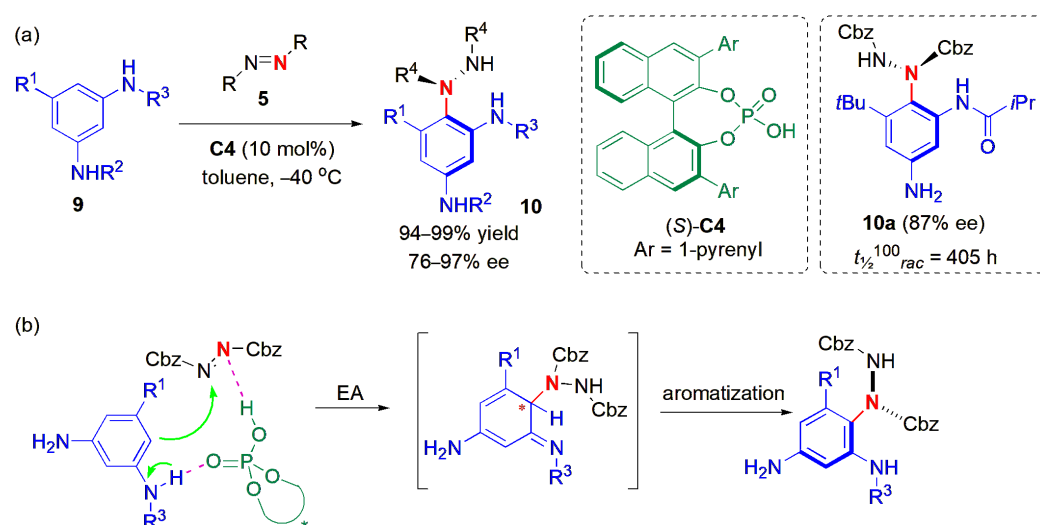


**Figure 5.** (a) Atropselective synthesis of C-N atropisomers through direct asymmetric aminations of 1,3-benzenediamines [38] and (b) the proposed mechanism.

Electrophilic addition facilitated by dual H-bonding interactions followed by an aromatization (in which there is central axial chirality transfer) has also been reported to be involved, as shown in Figure 5b. Contrary to the report on the amination of naphthylamines, in this case, benzyl chloroformate (Cbz)-substituted azodicarboxylates were more efficient in providing the desired stereoselectivity than Boc-substituted ones. The yields varied within the range of 94–99%, except in the case of a NHPH-substituted benzenediamine. A large range of electron-withdrawing  $R^3$  substituents could be used, as well as 5-substituents, and the products were obtained in high yields and ees. However, the configurational stability of products with  $R^1$  = primary alkyl groups was relatively low compared to that of the 5-*t*Bu-substituted products, presumably due to the lower steric hindrance provided by these groups. The highest stabilities were observed in *N*-acyl substituted products bearing a 5-*t*Bu and 3-NH<sub>2</sub> substituents (with  $t_{1/2}$  ranging from 226 to 405 h at 100 °C), e.g., as for **10a**.

The reaction of azonaphthalines **11** with *N*-arylcarbazoles **12** in the presence of chiral phosphoric acid **C3** also gave rise to axially chiral products (**13**) in an atropselective manner with excellent ees (Figure 6) [39]. The work by Li, Tan, and co-workers was inspired by the fact that *N*-arylcarbazoles are one of the most widely used host materials for OLEDs, due to the fact that they may display high triplet energies and competitive hole transport abilities. These properties often drive research towards obtaining new structurally diverse *N*-arylcarbazoles, with the aim of obtaining materials with good properties. The method developed in this study was compatible with a wide range of substituents in the starting materials, with ees remaining within 87 and 94%, with electron-donating or electron-withdrawing substituents in the aromatic rings. In addition, the reaction of the azonaphthalines with indoles **14** was also explored, allowing the synthesis of various C-N axial compounds **15** with ees up to >99%, although in this case, the reaction worked better with a different chiral phosphoric acid, **C5**.

Double enantioselective arene C-H amination reactions were also performed, although more forcing conditions were required in this case; reactions at 50 °C for 7 days allowed good yields of compounds **16** to be obtained, although this change did not affect the ees much. A different catalyst, **C6**, performed better in this case. The new products contain two chiral *N*-aryl axes.

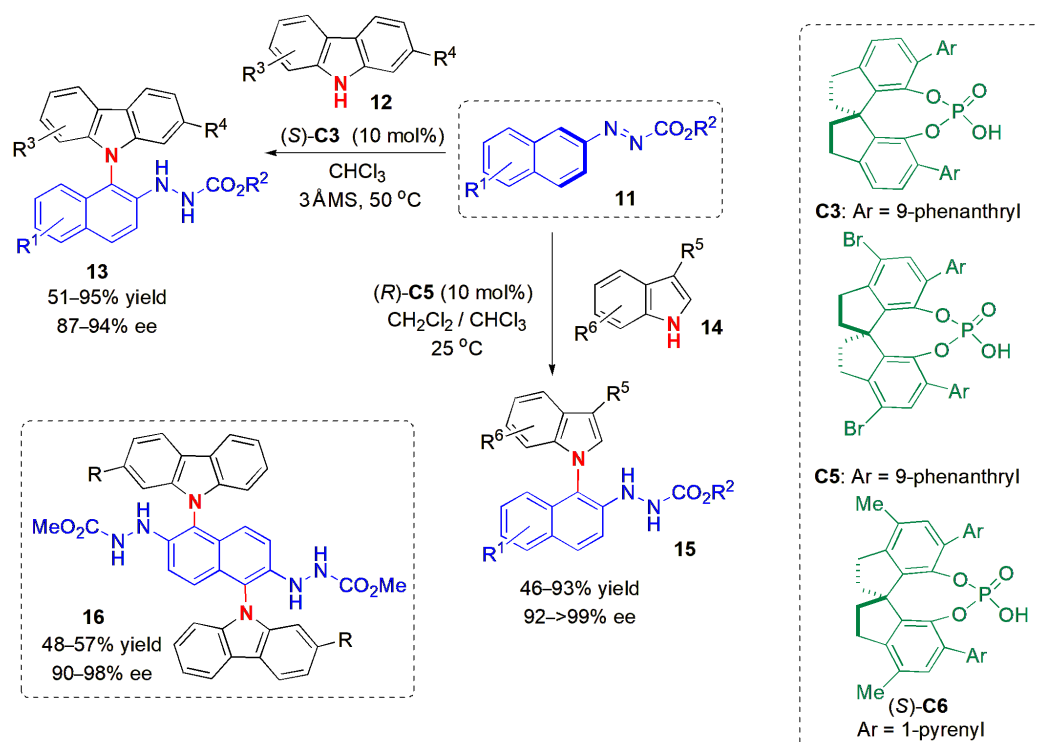


**Figure 6.** Atroposelective C-H arene amination [39].

## 2.2. N-H Functionalization

The first organocatalytic asymmetric synthesis of optically active axially chiral *o*-iodoacrylanilides and *N*-allyl-*o*-iodoanilides from compounds **17** and bromides was described by Maruoka and co-workers in 2012 [40]. *O*-iodoanilides **19** were obtained via phase-transfer catalyzed *N*-alkylation with organocatalyst **C7**, an organocatalyst that is itself also axially chiral (Figure 7). The presence of bulky extended aromatic *ortho*-substituents and *n*-hexyl groups on the binaphthyl-modified chiral ammonium salt were crucial for high ees to be obtained, alongside a low temperature of  $-20\text{ }^{\circ}\text{C}$ . The X-ray crystal structure of one product helped to indicate a mechanism of the reaction, suggesting that the catalyst can recognize the steric difference between iodide and methyl groups as *ortho*-substituents on the anilide, thus favoring a halide approach, preferentially, to one side of the aromatic ring rather than the other. Very high enantiomeric excesses (ees) were obtained, as determined by chiral HPLC analysis.

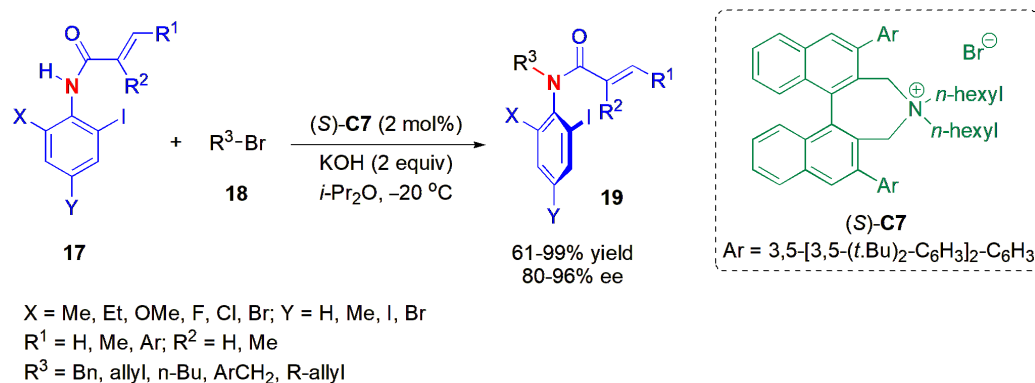


**Figure 7.** Atroposelective synthesis of axially chiral *o*-iodoanilides using phase-transfer catalyzed alkylations [40].

A similar N-H functionalization strategy was used by Li and co-workers to obtain axially chiral anilides, but via a Morita–Baylis–Hillman (MBH) reaction [41]. A biscinchona

alkaloid catalyst (**C8**) allowed the introduction of several acyl groups, e.g., substituted phenyl, naphthyl, alkyl, enyl, styryl, and benzyl, on the amide with very good yields, moderate to excellent *cis:trans* ratios, and good to excellent ees (Figure 8). Gram-scale syntheses were also possible. However, the allylation products **22** could not be separated using column chromatography or using HPLC. Hence, they were reacted with  $\text{CH}_2\text{N}_2$ , generating a cycloaddition product **23** easily within 5 min, the isomers of which could be isolated using column chromatography to help to confirm the ee. Racemization experiments performed in isopropyl alcohol at 80 °C showed that not only the steric hindrance, but also the electronic properties and the position of substituents, had an effect on the stereochemical stability of the products **22**, e.g., as for **22a–22c**.

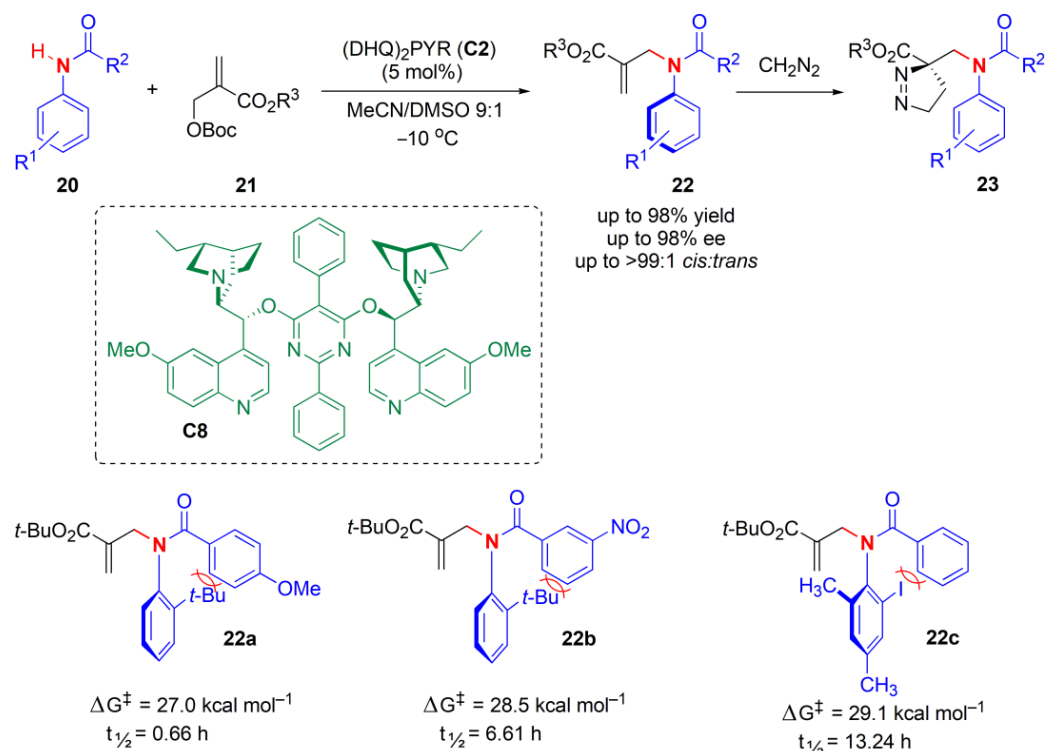


**Figure 8.** Atropselective Morita–Baylis–Hillman reaction for the synthesis of axially chiral anilides [41].

Although axially chiral anilides are a class of compounds that are emerging as biologically active scaffolds, their synthesis is complicated due to low rotation barriers. It has been noted previously that the presence of a heteroatom in the axis of rotation often causes a decrease in the rotational barrier [21]. In 2020, Li and co-workers reported a procedure to obtain axially chiral phosphamides **25** via an atropselective *N*-allylic alkylation reaction of phosphamides **24** and MBH carbonates **21** (Figure 9) [42]. The cinchona alkaloid hydroquinidine (**C9**) was an efficient catalyst for this atropselective strategy, and the products **25** were obtained in good yields and high ees. A good linear correlation was found to exist between the ees and the Charton values ( $R^2 = 0.91$ ), parameters which are commonly used to describe the steric hindrance of substituents [43]. From this linear free energy relationship analysis, it could be seen that substrates with large steric substituents, such as *t*Bu and Ad, gave better ees. However, steric hindrance was not the only factor at play, since when an *i*Pr group was present in the aromatic ring (at an *ortho* position), a sharp decrease in ee also occurred. Hence, the nature of the substituents was also a significant factor. Higher ees were obtained when a halogen atom was present at this position, suggesting the possibility of a halogen bonding interaction between the substrate and the catalyst, which helps to improve the ees.

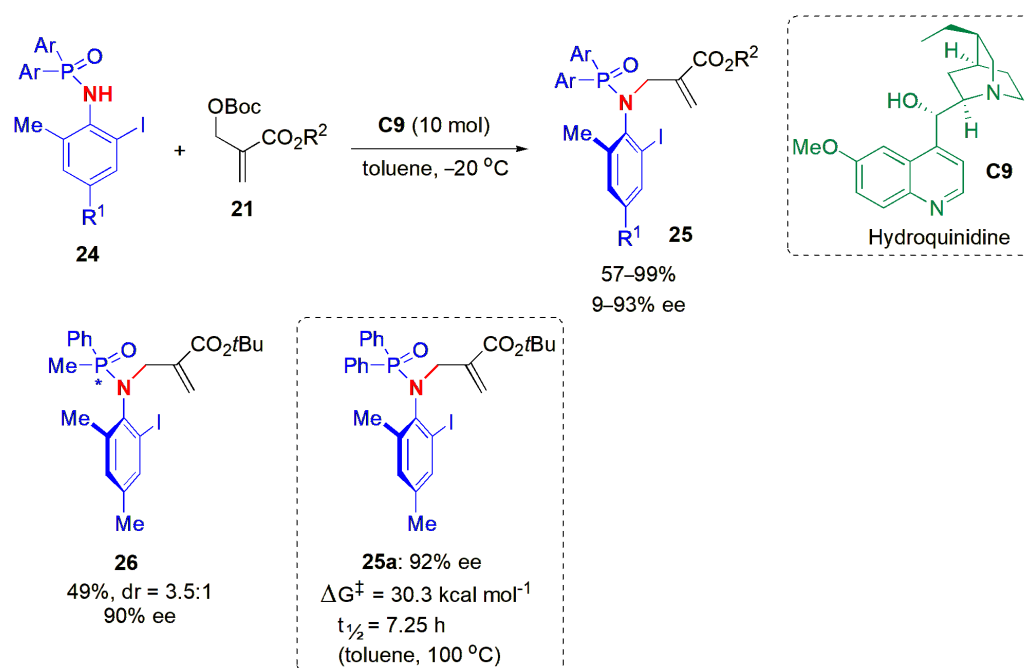


**Figure 9.** Synthesis of axially chiral phosphamides via atroposelective *N*-allylic alkylation [42].

A dissymmetric phosphamide was also used in an attempt to obtain a product with two different types of stereogenic elements, and indeed, the desired product **26** could be obtained in 49% yield (dr = 3.5:1, 90% ee) through a kinetic resolution process. This seems to be the first example of the synthesis of compounds containing both a *P*-stereogenic center and C-N axial chirality.

Racemization experiments with **25a** showed that the barrier to rotation was high. The potential of the newly synthesized compounds to act as chiral hypervalent iodine(III) catalysts was also demonstrated with the asymmetric oxidative dearomatization of phenol, and in Kita's reaction, i.e., the asymmetric oxidative spirolactonization of phenol derivatives.

### 2.3. C-H Functionalization and Related Approaches

Miller and co-workers instead chose an atroposelective C-H functionalization strategy to obtain axially chiral products [44]. In the presence of a tertiary amine-containing  $\beta$ -turn peptide (**C10**), 3-arylquinazolin-4(3*H*)-ones (quinazolinones) **27**, which are of pharmaceutical interest, could be brominated with high levels of stereoselectivity to yield compounds **28** (Figure 10). Screening experiments with a range of peptides suggested that the peptide  $\beta$ -turn secondary structure is important to achieving high ees in this reaction. The slow addition of NBS also helped to raise the ees. A broad range of substrates **27** with different substituents on the quinazolinone aromatic ring, at C-2 and on the *N*-Ar ring, were compatible with the reaction conditions, with the products **28** being obtained in high yields and very high ees. These products were isolated after phenol methylation with (trimethylsilyl)diazomethane, and acetic acid addition as the reaction's quench material. Mechanistic studies suggest that the initial bromination is achieved in the stereodetermining step, with the major monobromide intermediate, an *ortho*-substituted isomer, being atropisomerically stable. Evidence for this came from an experiment with peptide **C11** (Boc-Dmaa-D-Pro-Acpc-Val-NMe<sub>2</sub>) as a catalyst, which provides the opposite sense of induction to **C10** when the reaction is explored at the early stages (low conversion). The major product obtained was the *ortho*-monobrominated product, with a configuration opposite to that of **28**, which means that the stereodetermining bromination event is the first bromination to give **29**. The barrier to rotation about the chiral axis in **29** was calculated to be 35.5 kcal mol<sup>-1</sup> using DFT calculations, corresponding to a half-life of  $1.13 \times 10^{13}$  s. Further transformations of products **28** or **29**, e.g., by a dehalogenation Suzuki–Miyaura cross-coupling sequence to

*ortho*-arylated derivatives, and a regioselective Buchwald–Hartwig amination procedure to afford a *para*-amine substituted quinazolinone, proceeded with retention of configuration.

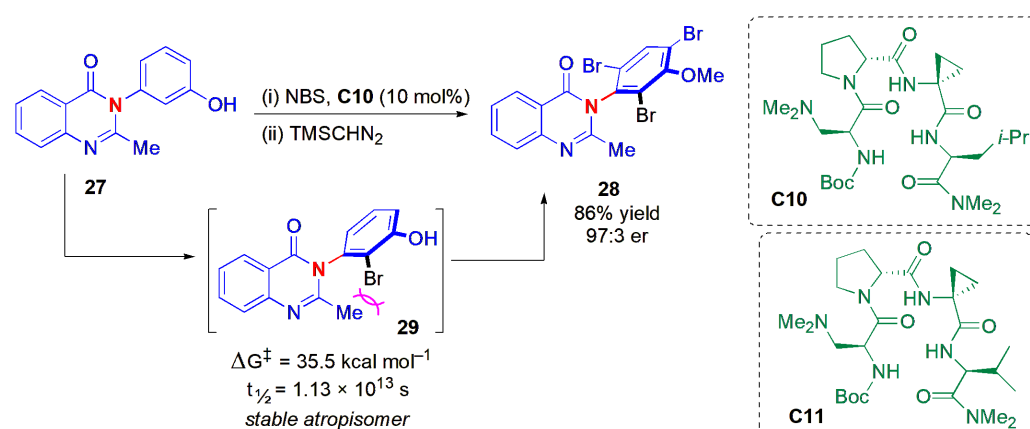


**Figure 10.** Enantioselective atroposelective bromination of arylquinazolin-4(3H)-ones [44].

Stereochemically stable diarylamines and related substances are few in number, because their axes typically possess lower stereochemical stabilities. In 2020, Gustafson and co-workers described the CPA-catalyzed atroposelective electrophilic halogenation of *N*-aryl quinoids **30**, which afforded diarylamine-like scaffolds **31** in an atroposelective manner for the first time (Figure 11) [45]. The resulting *N*-aryl quinoids possess a five-membered intramolecular N–H–O hydrogen bond that stabilizes them, with barriers to racemization approaching and exceeding 30 kcal mol<sup>−1</sup> ( $t_{1/2}$  (37 °C) > 4.5 years) in both protic and aprotic solvents, e.g., as **31a**. They are therefore considered sufficiently stereochemically stable for drug development [45]. High yields and ees were obtained for a variety of substrates. However, the aryl groups played an important role; if they were replaced by Me, a large drop (by more than 60%) in ee took place. When the aryl groups contained *ortho*-fluorine substituents, ees greater than 90% were observed. Fused ring systems, e.g., naphthyl, benzofuran, and benzothiophene, reacted to provide products in very high yields and ees up to 90%.

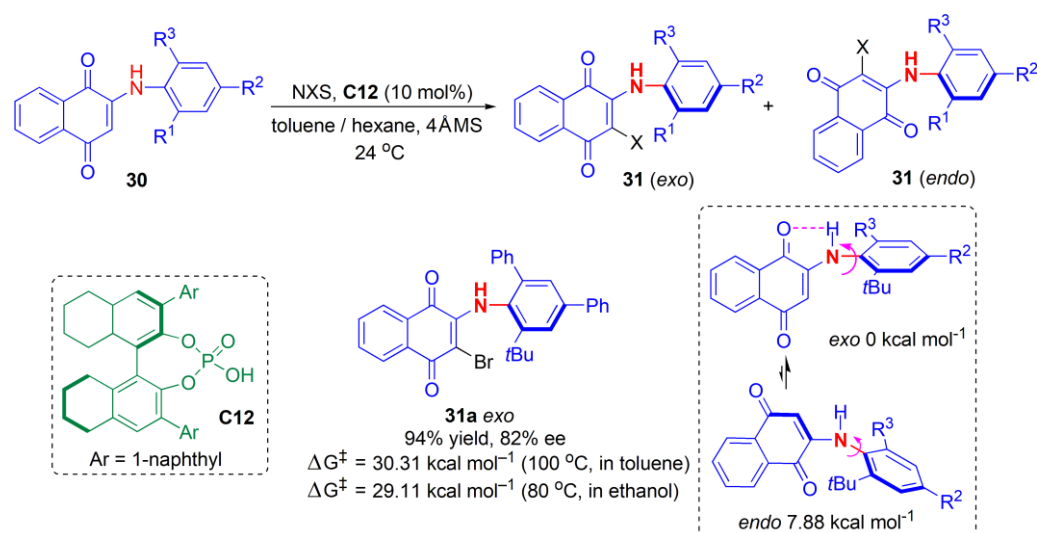


**Figure 11.** Atroposelective synthesis of *N*-aryl quinoid compounds [45].

Modifications of non-aromatic rings incorporating the C–N axis of symmetry have also been used to restrict rotation and allow the formation of distinct rotamers. An atroposelective electrophilic sulfenylation of *N*-aryl aminoquinone derivatives **32** was achieved for the first time in 2022 [46]. This development brings us one step closer to control of

axial chirality in diarylamines, which are useful structures in drug discovery; although they may possess two contiguous atropisomeric C-N axes, they are less stable, and their rotational barriers are not sufficiently high to prevent racemization. In order to achieve atropselectivity in the related *N*-aryl aminoquinone derivatives, Xue, Chen, and co-workers introduced an hydrogen acceptor sulfide group in the quinone ring, aiming to obtain an intramolecular N-H-S bond capable of locking one of the C-N axes into a planar conformation, in a manner similar to the example above, e.g., **34a** in Figure 12a. Sulfonylating reagent **33a** in combination with the new CPA (*S*)-**C13** afforded products **34** in very high yields and ees, irrespective of the nature of the substituents on the aryl ring. The quinone substituents could also be varied, but lower yields and ees were obtained in these cases. When benzofuran groups were present as substituents at the phenylamine moiety, a very low ee of 16% was also obtained.

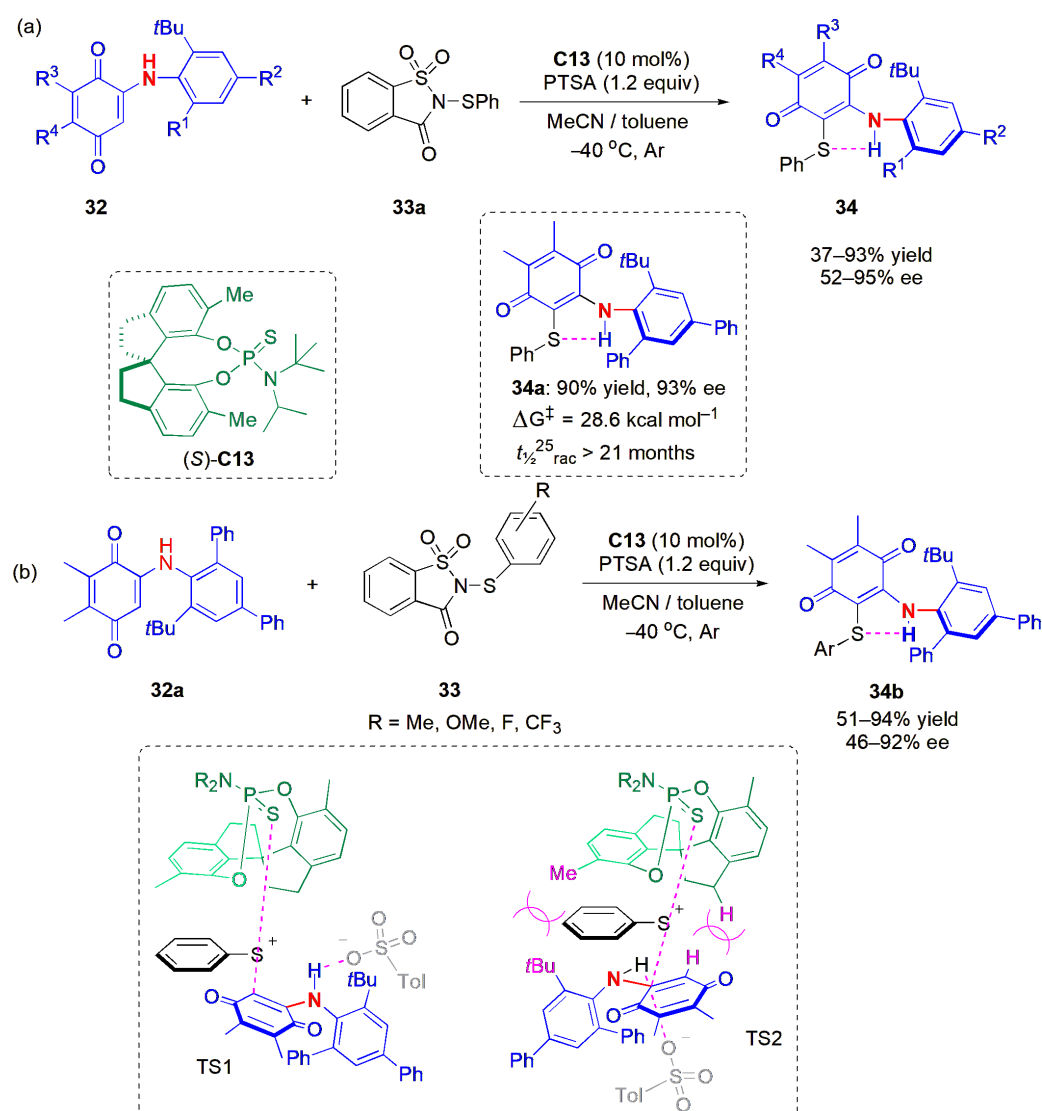


**Figure 12.** Atropselective electrophilic sulfonylation of *N*-aryl aminoquinone derivatives with sulfonylating reagent **33a** (a) and with a range of reagents **33**, as well as the transition states proposed (b) [46].

Different sulfonylating agents **33** were tried, within which the aryl group was varied and the products, e.g., **34b**, were obtained with moderate to good yields and moderate to high ees (Figure 12b). Steric hindrance caused by this group, as well as its nature, affected enantioselectivity. Electron-poor substituents in the aromatic ring improved the reactivity and hence the yields, as well as the ees in relation to aryl groups bearing electron-donating groups, which not only afforded products with lower ees, but also meant that the reactions

had to be performed at higher temperatures. The reaction was also tried on a *N*-methyl protected substrate, but no product was obtained in this case.

The energy barrier to racemization of **34a** was found to be approximately  $28.6 \text{ kcal mol}^{-1}$  ( $t_{1/2}^{25} \text{ } ^\circ\text{C}_{\text{rac}} > 21 \text{ months}$ ) in toluene; thus, **34a** is considered to be stereochemically stable [4]. DFT calculations were also performed, and revealed the origin of the atropselectivity. It was found that the key factor is the presence of strong steric repulsions between the catalyst's methylene unit on the spirocyclic skeleton and the methyl and *tert*-butyl substituents on the aromatic ring and the substrate's quinone group, respectively, which mean that TS1 is favored over TS2. This is in agreement with the fact that when the N atom is methylated, there is no reaction.

#### 2.4. Desymmetrization

Enantioselective desymmetrization reactions provide another approach for the introduction of axial chirality. *N*-(2-*t*-butylphenyl)succinimides **35** were subjected to a desymmetrization reaction, through a vinylogous Michael addition of 3-substituted cyclohexenones **36** by Bencivenni and co-workers in 2014 (Figure 13) [47]. In the presence of cinchona alkaloid **C14**, the reactions proceeded in an enantioselective fashion, with remote control of the axial chirality, to afford atropisomeric succinimides **37** and **38** with two adjacent stereocenters. The utilization of *N*-Boc-*L*-phenylglycine **C15** as a co-catalyst helped to raise the ee.

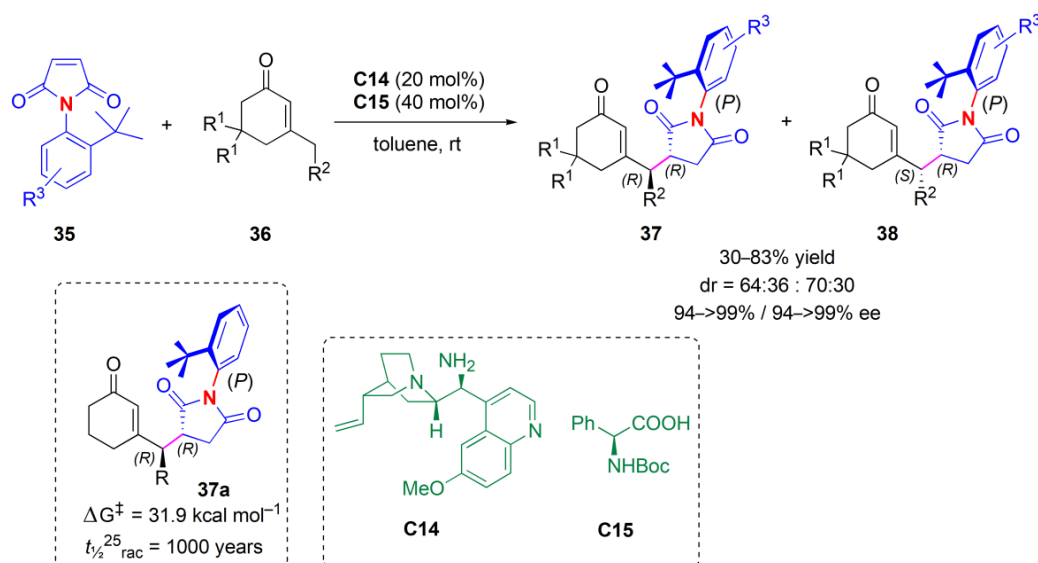


**Figure 13.** Aminocatalytic desymmetrization of *N*-arylmaleimides via vinylogous Michael addition [47].

The ees were very high, although the diastereoselectivity was moderate. A *P,R,R* and a *P,R,S* absolute configuration were assigned to the major and minor diastereoisomers obtained, based on X-ray diffraction and EDC spectra experiments. The scope of the reaction was examined with different substituents on the *N*-aryl ring, and it was found that when halogen, phenyl or methoxy substituents were present, and with an amino group, the yield and ees were high. On the contrary, the presence of a second *t*-butyl group at position 5 of the maleimide aromatic ring resulted in only traces of products, and with ortho- iodo-, triethylsilyl- or phenyl groups, the products have chiral axes that quickly epimerize at 25 °C. Enones with various substituents were also tried; the most effective ones were methyl and isopropyl.

The thermal stability with respect to the epimerization of the chiral axis was also probed. When **37a** was heated to 130 °C in  $\text{C}_2\text{D}_2\text{Cl}_4$ , 10 h later, an equilibrium ratio of 62:38 and a new diastereoisomer were observed. The fact that this new compound was indeed a rotamer and not another diastereoisomer was confirmed using NMR analysis and an

NOE experiment. The energy barrier to rotation was found to be  $\Delta G_{\text{epi}}^{\ddagger} = 31.9 \text{ kcal mol}^{-1}$ , corresponding to a  $t_{1/2}^{25} = 1000$  years.

The Bencivenni group developed soon after a formal Diels–Alder reaction of enones **39** catalyzed by a primary amine **C14** to achieve an atroposelective desymmetrization of *N*-arylmaleimides **35** (Figure 14) [48]. 1-Hydroxy-2-naphthoic acid (**40**) worked well as an additive. The product succinimides **41** were obtained as single diastereoisomers (*dr* > 19:1 in all cases) in good yield and excellent ees with either cinchona alkaloid derivative **C14** or **C16**, **C16** giving the opposite enantiomers of **C14**. Electron-withdrawing and electron-donating substituents could be used, but the reactivity was suppressed completely by an *o*-bromo substituent in the aryl group of the enone, and also when an alkyl chain and an ester substituent were used. Similarly, when 5-*t*Bu and 5-NO<sub>2</sub> substituents were employed in the *N*-Ar group, no product was obtained. The chiral axis is generated under catalyst remote control. The stereochemical outcome depends on the way that the  $\alpha,\beta$ -unsaturated enamine, produced by the reaction between the catalyst and ketone, and the maleimide, approach one another. The unsaturated enamine approaches from the maleimide side that is not shielded by the *tert*-butyl group in the TS. Both central and axial chirality are created in this example.

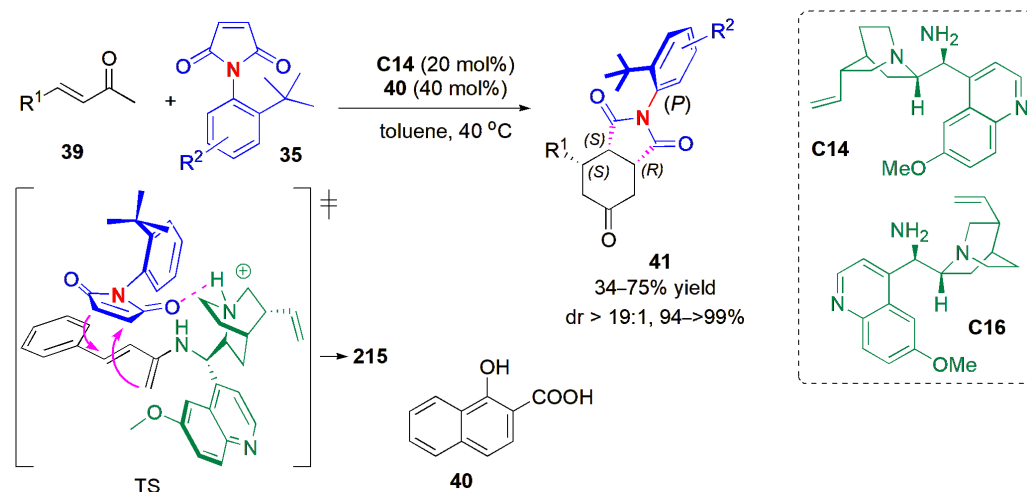


**Figure 14.** Organocatalytic atroposelective formal Diels–Alder desymmetrization of *N*-arylmaleimides [48].

When instead of  $\alpha,\beta$ -unsaturated ketones, the corresponding enals **42** are used to react with maleimides **35** in the presence of a secondary amine, **C17**, *N*-substituted phthalimides **43** are produced in an atroposelective desymmetrization reaction (Figure 15). This *de novo* arene construction, proceeding through an oxidative [4 + 2] cycloaddition, was described by Mondal and Mukherjee in 2022 [49]. The dienamine catalysis obtained allows the formation of products in very high ees, using remote stereocontrol via the *endo* TS. Only axial chirality is produced in this example. The highest yields were obtained when R<sup>3</sup> = NO<sub>2</sub> and R<sup>2</sup> was an electron-donating group, and the lowest ee was achieved with a 2-Me substituent, when R<sup>3</sup> = NO<sub>2</sub>. When R<sup>3</sup> = H, only an 11% yield was obtained, even after 11 days. Thus, the nitro group has a large effect on the reactivity.

Another example of the use of a desymmetrization strategy to obtain axial chirality was described by Jindal, Mukherjee, Biju and co-workers in 2021 [50]. In this case, *N*-aryl maleimides **35** were subjected to an intermolecular Stetter reaction/oxidation sequence (Figure 16). Although no reaction could be observed with 4-chlorobenzaldehyde, phthalaldehyde **44** afforded good yields of products **45** with high ees when reacted in the presence of the chiral *N*-heterocyclic carbene (NHC) **C18** and Hünig's base, followed by *in situ* oxidation of the resulting product with pyridinium dichromate (PDC). Overall, the products are formed via a tandem intermolecular Stetter reaction followed by an intramolecular aldol reaction, with subsequent oxidation. Product stability was inspected by heating **45a** (R = H)

in toluene. Up to 90 °C, the ee was preserved, but at 110 °C, the ee dropped to 84%. With a further increase in temperature, the ee dropped even more, being almost racemic at 150 °C, suggesting that there was unrestricted rotation of the C-N bond at this temperature. The  $\Delta G_{\text{rot}}^\ddagger$  for the C-N bond in **45a** was calculated to be 32.4 kcal mol<sup>-1</sup>, using DFT studies. In this study, the *ortho*-*tert*-butyl group present in the *N*-aryl substituents played an important role in restricting the rotation about the C-N axis. When replaced with a dimethyl phenyl group, the ee of the reaction product was still high (43% yield, 86% ee); however, if this group was replaced with an isopropyl group, the ee dropped to 60%.

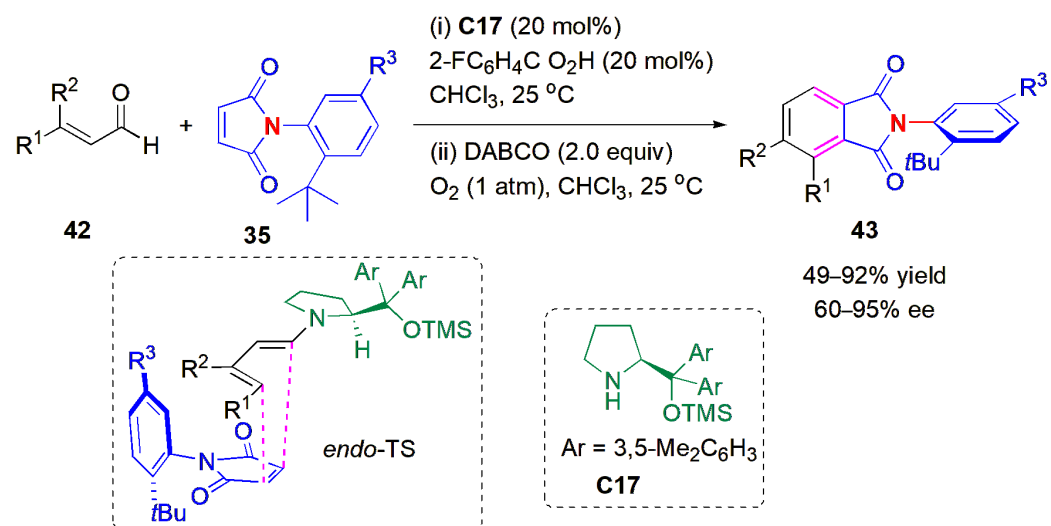


**Figure 15.** Atropselective desymmetrization reaction leading to phthalimides [49].

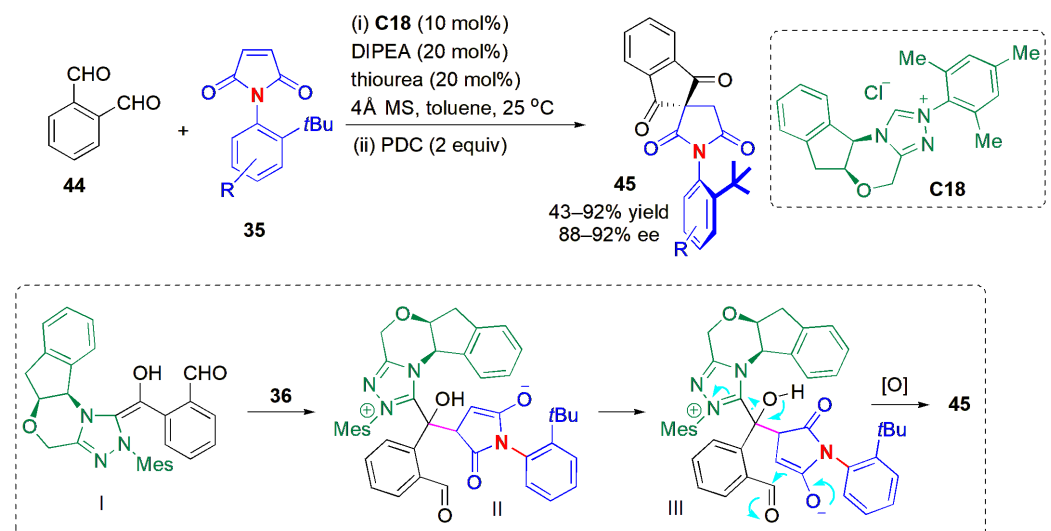


**Figure 16.** Atropselective synthesis of *N*-aryl succinimides via an NHC-catalyzed desymmetrization of *N*-aryl maleimides [50].

An organocatalytic tyrosine click-like reaction allowed the synthesis of axially chiral urazoles [51]. Zhang et al. found that by using a bifunctional thiourea-based catalyst (**C19**), efficient discrimination of the two reactive sites in the triazolidione ring of substrates **46** could be achieved upon reaction with phenols **47** or naphthols **48**, and the stereochemical information of the catalyst could be transferred into axial chirality at a remote position, far from the reactive site, in the urazoles (Figure 17). The reactions proceeded readily at a low temperature (−78 °C), and high yields and ees of products **48** or **50**, respectively, were obtained for a variety of substrates bearing electron-withdrawing or electron-donating substituents at different positions in the aromatic rings. To probe the configurational

stability of the products, a solution of product **45a** ( $R^1 = 2\text{-}t\text{Bu}$ ) in toluene or MeCN was heated at 80 °C for 12 h. Chiral HPLC analysis showed that there was no difference in the ee values of **13a**, confirming its stability. Similar reactions were performed with indoles **14** as desymmetrization reagents, but a different catalyst was required. In this case, chiral phosphoric acid (CPA) **C3** was an efficient catalyst, and the corresponding products **51** were obtained with very high yields and ees. Gram-scale reactions could be performed successfully, with no loss of enantioselectivity.

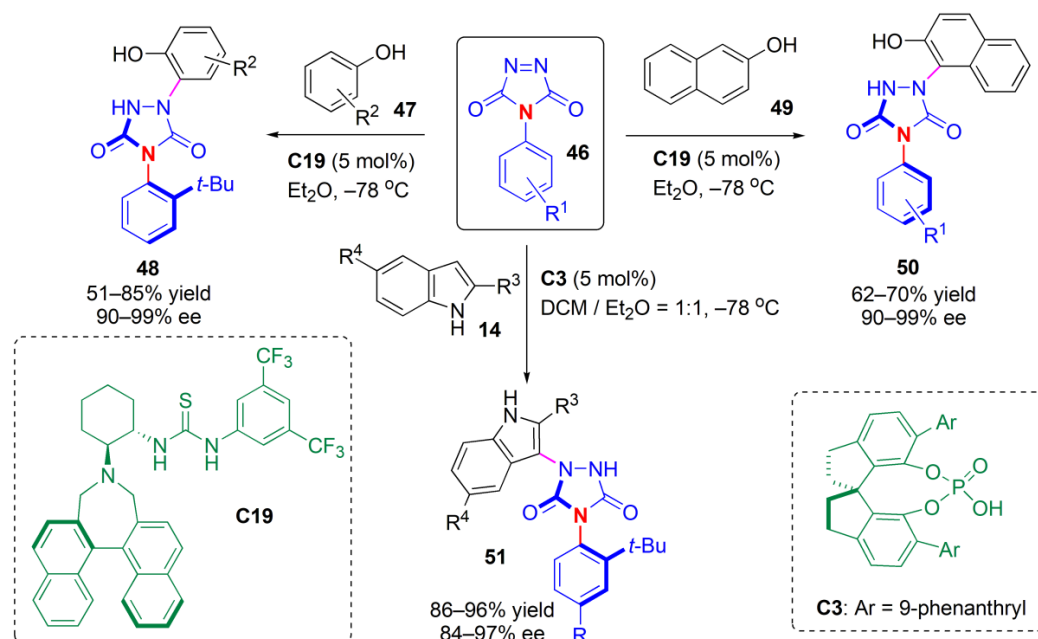


**Figure 17.** Enantioselective synthesis of axially chiral urazoles [51].

Inspired by the studies in the desymmetrization of maleimides, Tan and co-workers studied a way to desymmetrize arylpyrroles **52** and reported the results in 2019 [52]. Axially chiral arylpyrroles are core structures of a wide range of natural products and pharmaceutical agents [53,54]. Chiral arylpyrroles are also present in chiral ligands; some are chiral catalysts and even chiral resolving agents. Until this report, chiral resolution or chiral chromatography was used to obtain axially chiral arylpyrroles in an optically pure state. In this work, enantioenriched axially chiral arylpyrroles were obtained either by means of organocatalytic atroposelective desymmetrization, or by kinetic resolution in the case of nonsymmetrical pyrroles (Figure 18). Depending on the remote control of chiral catalyst, the arylpyrroles were obtained in high yields and excellent ees under mild reaction conditions. As an electrophilic reagent, diethyl ketomalonate **53a** was selected, and CPA (*S*)-**C20** was found to be the best catalyst. In this case, not only did the *tert*-butyl group serve as an efficient *ortho* substituent on the *N*-aryl ring to hinder rotation, but high ees were also obtained with a range of other functional groups (Figure 18). The nature of a 4-substituent did not matter either. Similar results were also obtained with other malonates, e.g., *i*Pr, *t*Bu). More critical to the atropselectivity (and also to the yield) was the nature of the substituents at the 2-position in the pyrrole ring. When a change was introduced in the pyrrole ring via replacement of the substituent at C-2 with another different from methyl, the system was no longer symmetric. The products could be obtained using the same catalyst with high selectivity, irrespective of the nature of the substituent (electron-withdrawing or electron-donating), via kinetic resolution, with a good to high selectivity factor ( $S = 32\text{--}69$ ). The absolute configuration of one product, **55a** ( $R^1 = \text{Me}$ ,  $R^2 = t\text{Bu}$ ,  $R^3 = \text{H}$ ,  $R^4 = i\text{Pr}$ ) was determined using X-ray crystallographic analysis to be (*aS*), and those of the other products were assigned by analogy.

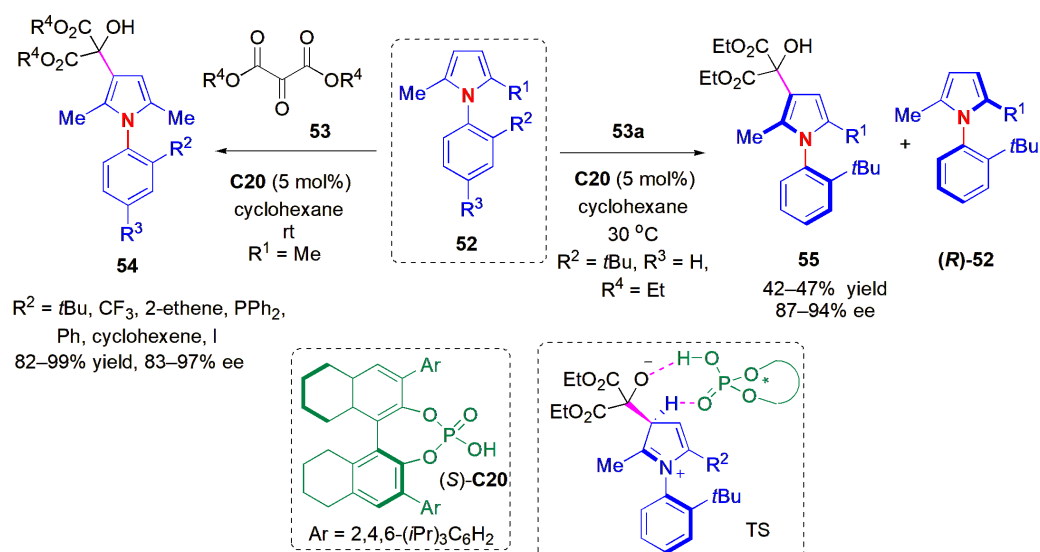


**Figure 18.** Atroposelective synthesis of axially chiral arylpyrroles [52].

The configurational stability of the products was investigated by heating **55b** in different solvents (*i*PrOH, DCE, and toluene) at up to 150 °C for 24 h. Deteriorations of stereochemical integrity were negligible, even when the substrate began to decompose. It was assumed that the key interactions controlling the atropselectivity were hydrogen bonding between ketomalonate and the CPA to form a chiral pocket for the induction of chirality, and H-bonding with the second carbonyl group of the ketomalonate so as to fix the whole system in a rigid configuration, as in TS1. The diphenylphosphine derivatives were applied as ligands to palladium in enantioselective allylic substitution reactions, thereby affording products with high ees.

### 2.5. Annulation

The last general approach for the construction of C-N axially chiral molecules is atropselective annulation, i.e., *de novo* ring construction, in which at least one ring is built up. In this context, enantiomerically pure aryl pyrroles were synthesized for the first time, by Tan and co-workers, using an atropselective method based on a catalytic asymmetric Paal–Knorr reaction, in 2017 [55]. A functionalized 1,4-diketone **56** was reacted with an aryl amine **57** in the presence a combined-acid catalytic system consisting of a Lewis acid, ferric triflate, and chiral phosphoric acid **C21** (Figure 19). The products were obtained in high yields and ees. The presence of electron-withdrawing groups on the aromatic substituent of the diketone favored yields and ees. The *ortho* group on the *N*-aryl ring was not only restricted to the *tert*-butyl group; the bromo, iodo, and phenyl groups at this position were well tolerated too, and the products could be obtained with high ees.

Control experiments to trap the intermediate allowed the isolation of species **B**, obtained from condensation product intermediate **A**, which confirmed that the reaction proceeds via an enamine intermediate. This is followed by acid-catalyzed dehydrative cyclization, which is a deviation from the usual Paal–Knorr reaction mechanism.

In the same year, Seidel and co-workers developed a catalytic enantioselective synthesis of isoindolinones **61** through the condensation of 2-acylbenzaldehydes **59** and anilines **60** (Figure 20) [56]. The reaction was catalyzed by a very low loading of CPA **C22** [(*S*)-TRIP] (1 mol%), and it was complete within 10 min. Products **61** with several substituent patterns were obtained in up to 98% ee. Anilines bearing an *ortho*-*t*-butyl group formed atropisomeric products through the simultaneous generation of axial and point chirality from two achiral substrates. The method was applied to the first catalytic enantioselective synthesis of the natural product mariline A. The highest yields were obtained with electron-rich benzaldehydes.

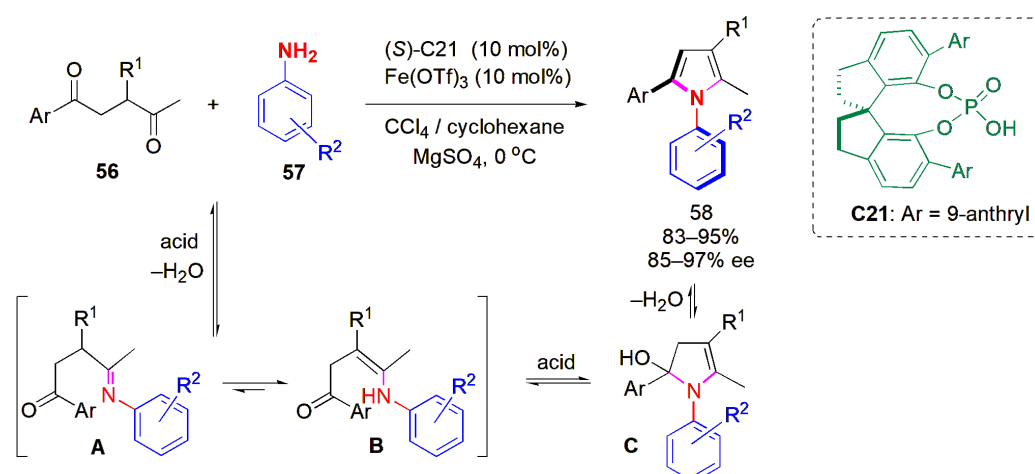


Figure 19. Atroposelective synthesis of arylpyrroles via a catalytic asymmetric Paal–Knorr reaction [55].

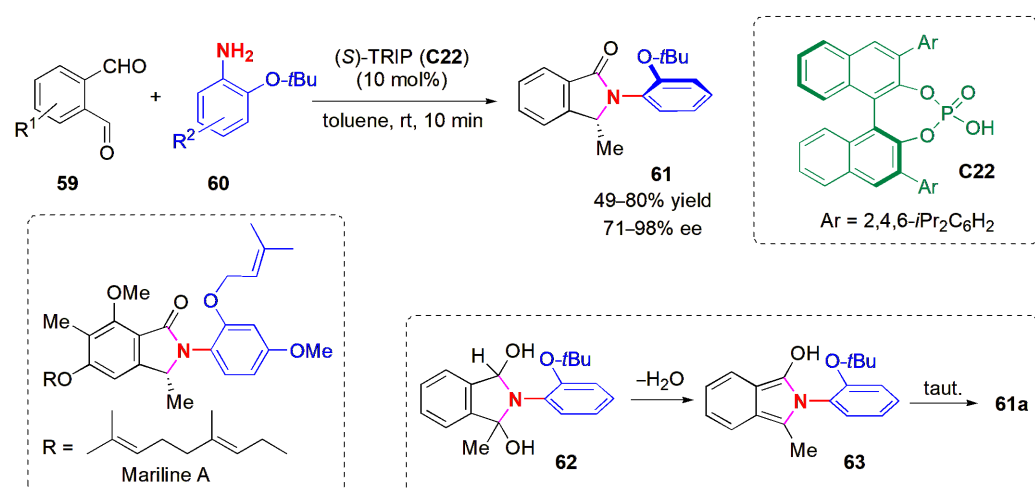
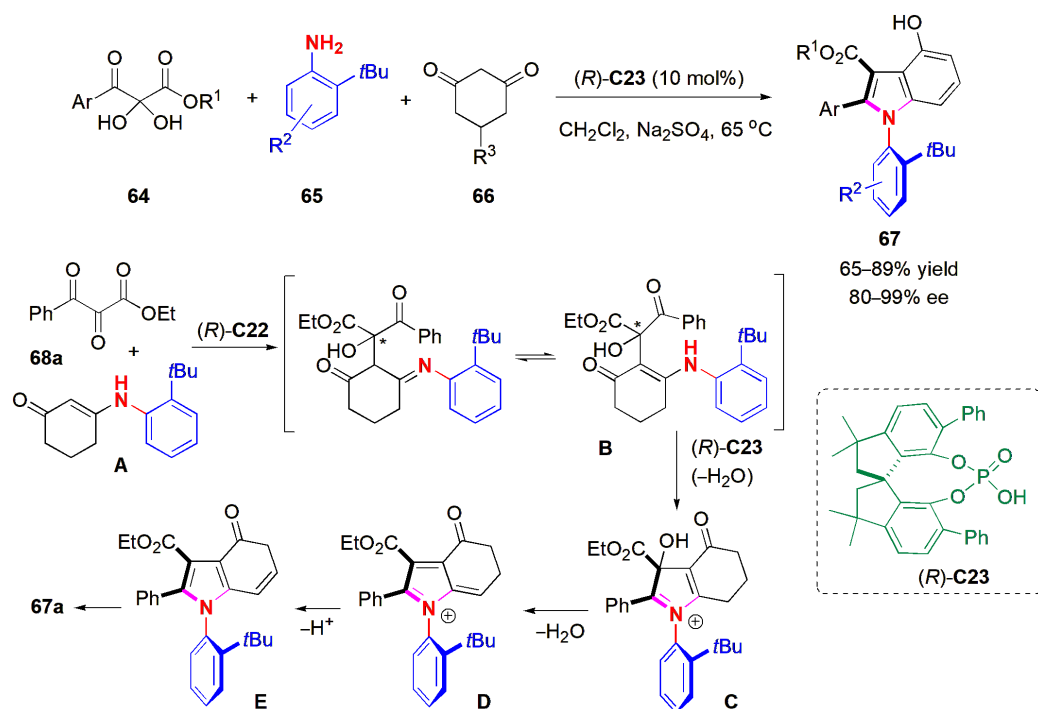


Figure 20. Catalytic enantioselective synthesis of isoindolinones 61 [56].

An organocatalytic atroposelective phosphoric acid-catalyzed three-component cascade reaction was utilized by Lin and co-workers to obtain axially chiral *N*-arylindoles [57]. 2,3-Diketone esters **64**, aromatic amines **65**, and 1,3-cyclohexanedione **66** reacted to provide a wide range of products **67** in high yields and very high ees (Figure 21). The authors proposed that the reaction proceeds via an intermediate enamine (**A**), which undergoes chiral acid-catalyzed aldol condensation with the dehydrated 2,3-diketone to produce **B**; it also undergoes dehydrative cyclization to generate **C**, dehydration via 1,4-elimination to produce **D**, and loss of acid to yield **E**, which tautomerizes to yield the final product. This multicomponent reaction was based on a previous report by the Doyle group, whose reaction was performed without a chiral catalyst and yielded racemic products [58].

The synthesis of six-membered rings showing atropisomerism has also been described using atroposelective methods involving de novo ring construction. One such method is the catalytic asymmetric construction of arylquinazolinones **70** from *N*-aryl anthranilamides (**69**) and benzaldehydes, as reported by Tan and co-workers in 2017 (Figure 22) [59]. CPA **C24** worked well in the presence of 2,3-dichloro-5,6-dicyano-1,4-benzoquinone (DDQ), despite the high steric hindrance imposed by the reactant molecules. Substrates bearing both electron-withdrawing and electron-donating substituents were well tolerated. At the same time, the atroposelective synthesis of alkyl-substituted arylquinazolinones **71** was also described, and achieved via a Brønsted acid-catalyzed carbon–carbon bond cleavage strategy. In this case, the desired product could not be obtained upon reaction with ketoesters, but when 4-methoxypentenone was used as reaction partner with a more

acidic catalyst **C25** in the presence of  $\text{MgSO}_4$ , several axially chiral methyl-substituted arylquinazolinones could be obtained in high yields and ees. Other diketones gave poorer results, which is a limitation of the method. It was also shown that the protocols could be applied to the asymmetric total synthesis of eupolyphagin, a natural product bearing a cyclic arylquinazolinone skeleton.



**Figure 21.** Atroposelective phosphoric acid catalyzed three-component cascade reaction to synthesize axially chiral indoles [57].

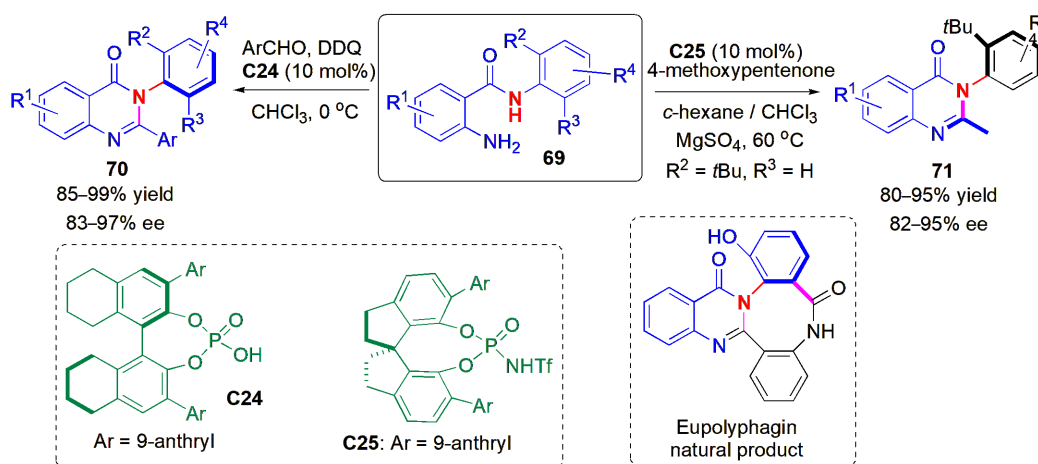


**Figure 22.** Atroposelective synthesis of axially chiral arylquinazolinones [59].

De novo ring construction was also adopted by Jin and co-workers to obtain thiazine derivatives with C-N axial chirality in 2021 [60]. An organocatalytic atroposelective cycloaddition reaction between thioureas **72** and ynals **73** was developed with an NHC [(*S*)-**C26**] as a catalyst. A wide range of chiral thiazine derivatives **74** could be obtained with good yields and excellent ees (Figure 23). In this reaction, the use of an additive, scandium triflate, helped to raise the yields, which dropped considerably (to below 40%) when the benzoyl group in the thiourea was replaced by *t*BuCO, or when the isopropyl *ortho*-substituent in **22** was replaced by a *tert*-butyl group. It was assumed that the reaction proceeded via the

formation of an intermediate acetylenic acylazolium intermediate from the reaction of the catalyst with **21**, which reacts to form a new form C(sp<sup>2</sup>)-S bond, producing intermediate **I**, followed by catalyst-controlled face-selective intramolecular lactam formation. The barrier to rotation determined by heating **74a** (98% ee) at 100 °C for 24 h in mesitylene was 29.5 kcal mol<sup>-1</sup> ( $\Delta G^\ddagger$ ), which agreed with the result calculated through density functional theory (DFT) ( $\Delta G^\ddagger = 30.4$  kcal mol<sup>-1</sup>). The thiazine ring is an important heterocyclic motif that is present in many medicines and agricultural chemicals; it is the structural element that is usually responsible for their bioactivity, e.g., the antibiotic cephalosporins such as cefradine, omonasteine, used in the treatment of respiratory diseases [61], and the pesticide buprofezin [62].

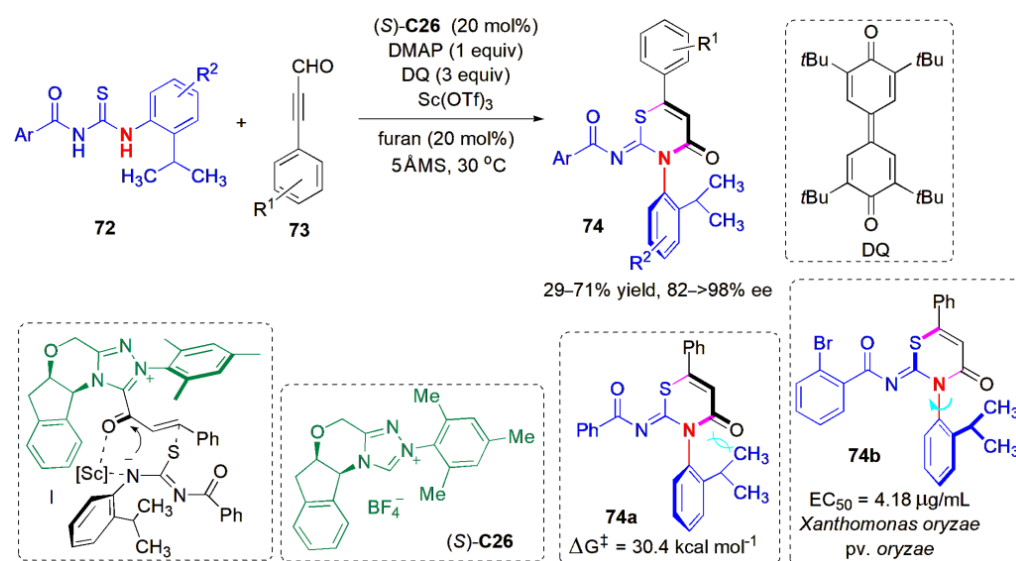


**Figure 23.** NHC-catalyzed atropselective annulation for the synthesis of thiazine derivatives **23** [60].

The authors also probed the biological activity of the new compounds. Indeed, they found that there was antibacterial activity against *Xanthomonas oryzae* *pv. oryzae* (Xoo), which causes leaf blight in rice plants [63]. Among bacteria-related plant diseases, rice bacterial leaf blight is still one of the most difficult diseases to control, and may cause significant damage [64]. In addition to resistant varieties, agrochemicals such as bismertiazol and zinc thiazole are also used. However, they are not completely satisfactory, and the pursuit of more efficient antibiotics is still an active area of research. The axially chiral thiazines **74** have shown promise as control agents, the most effective being (S)-**74b**, with an EC<sub>50</sub> value of 4.18 µg/mL, which is superior to the two agrochemicals mentioned above.

In a recent example of synthesis of enantioenriched heterobiaryl atropisomers, an imidazole ring was constructed to establish a new C-N axis of chirality (Figure 24) [65]. Hence, naphthylamines (glycine derivatives) **75** and nitrosobenzenes **76** were reacted by means of a domino approach to synthesize axially chiral *N*-arylbenzimidazoles **77**, with the catalysis provided by a chiral phosphoric acid (**C27**), with excellent chemo- and regioselectivity, as well as high levels of enantiocontrol. Different alkyl and cycloalkyl substituents on the nitrobenzene ring could be used successfully, but electron-withdrawing groups at this position (Cl, CF<sub>3</sub>) caused a considerable drop in yield; however, the ees were not affected much. Several glycine derivatives were compatible with the reaction conditions. The configurational stability of the products was studied with one example, **77a** (R<sup>1</sup> = OMe, R<sup>2</sup> = Me, R<sup>3</sup> = *i*Pr, 96% ee) by heating at 120 °C for 24 h. There was no loss in ee, but there was partial decomposition of the substance during this period. A plausible reaction mechanism is shown in Figure 24. Initially, there is the chemo- and regioselective nucleophilic addition of 2-naphthylamine **75a** to **76a**, enabled by dual CPA activation, to produce **A**. Dehydration of **A** leads to diimine **B**. **B** may be converted into **C** via a [1,5] hydrogen shift or through successive reduction/oxidation steps (not shown).

CPA-catalyzed intramolecular enantioselective addition of the amine to the imine provides the stereo-enriched annulated intermediate **D**, the stereoselectivity determination step in the domino reaction. Finally, oxidative aromatization of **D** produces the desired product **77a**.

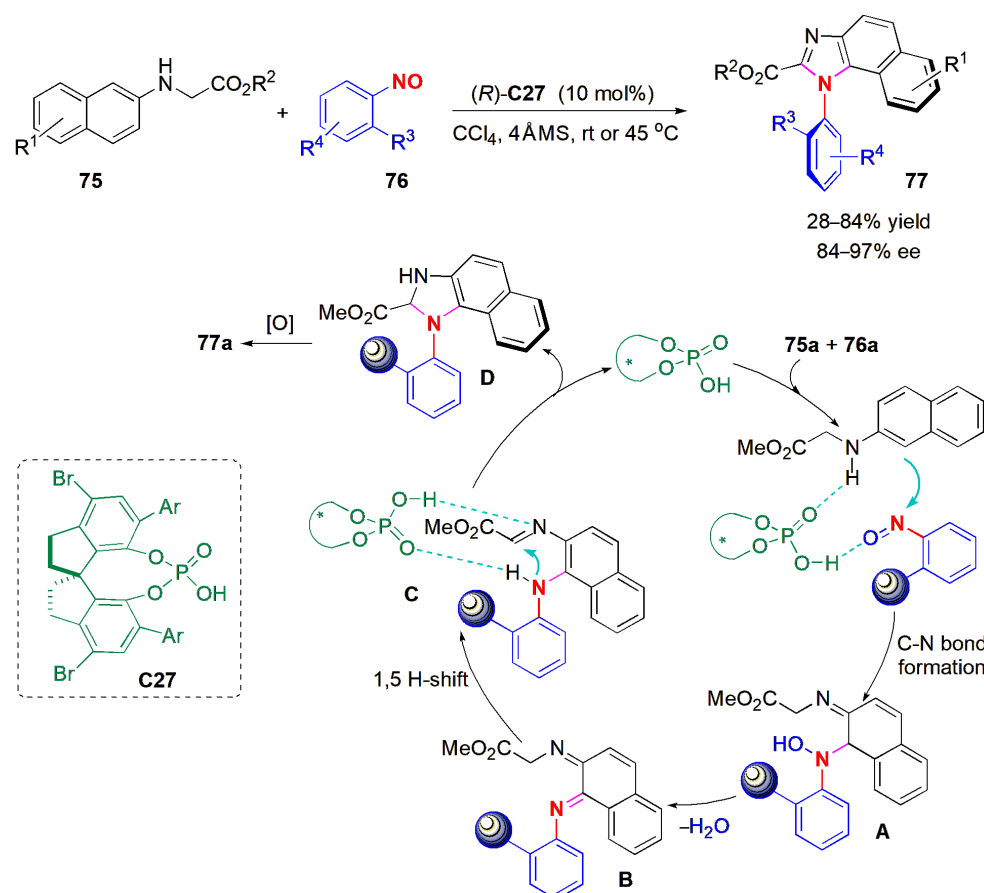


**Figure 24.** CPA-catalyzed enantioselective construction of atropisomeric *N*-arylbenzimidazoles [65].

An atropselective Pictet–Spengler reaction of *N*-arylindoles **78** was reported in 2021 [66]. Kwon and co-workers obtained *N*-aryl-tetrahydro- $\beta$ -carboline **79** with C-N bond axial chirality via dynamic kinetic resolution using a chiral phosphoric acid (**C27**) as catalyst (Figure 25). The organocatalytic version of the Pictet–Spengler reaction, an acid-catalyzed intramolecular Friedel–Crafts-type reaction involving iminium ions, was developed by List and co-workers in 2006 [67]. It is often applied to the synthesis of complex natural products, including  $\beta$ -carboline alkaloids [68], and although several asymmetric versions have been reported since 2006, the report by Kwon and co-workers was the first example of an atropselective synthesis of this class of compounds [64]. A wide range of substituents were compatible with the reaction conditions. The highest ees were obtained when benzaldehydes **80** were used as reaction partners instead of paraformaldehyde (all >99% ee). In these cases, both axial and point stereogenicity could be controlled. The ees were quite susceptible to the nature and number of the substituents on the *N*-aryl ring, with NHBn showing the highest ees, and NBN<sub>2</sub> the lowest (56% ee). The authors concluded that in the first case, the hydrogen bond donor substituent forms a secondary interaction with the phosphoryl oxygen of the catalyst, which helps to increase the stereoselectivity. The presence of a *meta*-substituent on this ring caused a further drop in ee. It was proposed that the reaction proceeded via the formation of an imine, itself resulting from the condensation of paraformaldehyde with the substrate, and dynamic kinetic resolution. The absolute configuration was determined via X-ray crystallography of the 4-bromobenzamide derivative of **81a** ( $R^1 = \text{H}$ ,  $R^2 = \text{Me}$ ,  $R^3 = \text{NHBn}$ ).

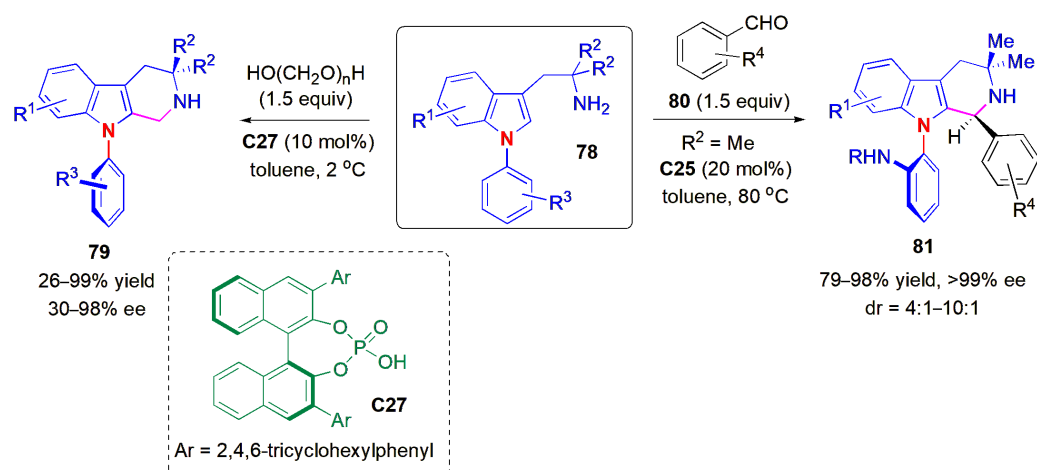


**Figure 25.** Atropselective Pictet-Spengler reaction for the synthesis of chiral *N*-aryl-tetrahydro- $\beta$ -carboline [66].

In 2022, Biju and co-workers described a procedure to obtain C–N axially chiral *N*-arylamino maleimides via kinetic resolution [69]. Hence, in the reaction between maleimides **82** and 2-bromoaldehydes **83**, performed in the presence of chiral NHC **C18**, [3 + 3] annulation with one of the enantiomers of maleimide takes place, and fused-dihydropyridinones (bearing axial/central chirality) up to 6:1 dr, >98% ee are obtained (Figure 26). The opposite enantiomer stays unreacted and is recovered with up to >98% ee. Remote chirality control is observed. The sense of induction is determined by a *Re* face addition of maleimide to the  $\alpha,\beta$ -unsaturated acylazolium. *Si* face addition (addition from the top) is hindered by both the *t*-Bu group and the aminoindanol moiety of the carbene. There was also remote chirality induction governed by the bulky *t*-Bu group of the maleimide substrate and the aminoindanol moiety of the NHC catalyst.

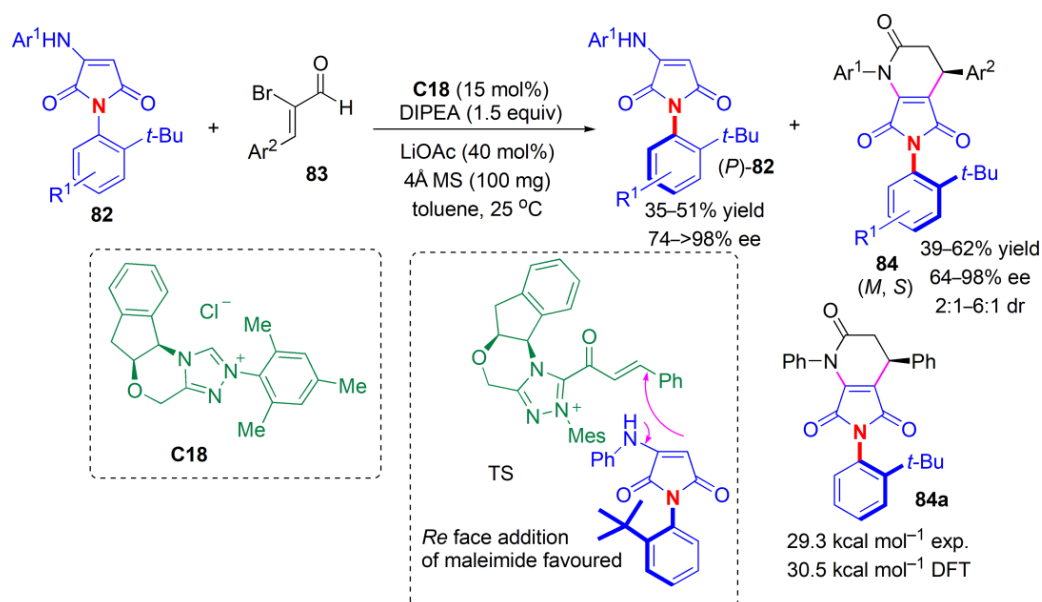


**Figure 26.** Kinetic resolution approach to the synthesis of C–N axially chiral *N*-aryl aminomaleimides [69].

### 3. N–N Axial Chirality

It was only in 2021 that the first method for the organocatalytic atropselective synthesis of N–N axially chiral compounds was described. However, the N–N bond is found widely in natural products, pharmaceutical agents, and organic materials. Based on the knowledge

that pyrrole, and quinazolinone rings have been found to be present in biologically active molecules containing N–N bonds, Houk and co-workers planned research involving these compounds, aiming to produce N–N axially chiral substances [32]. Indeed, they found that 1-aminopyrroles and 3-aminoquinazolinones could be synthesized in an atropselective manner, with high yields and excellent enantioselectivities. When starting from 1-aminopyrrole **86**, N–H functionalization via allylic alkylation with the Morita–Baylis–Hillman (MBH) adduct **85**, sufficient constraints were introduced to the N–N bond rotation, so that two non-interconvertible atropisomers were obtained **87** (Figure 27). If the reaction was performed in the presence of quinidine, high yields and ees of products **87** could be obtained for these pyrrole amides. Higher ees were obtained for pyrroles containing electron-rich aryl groups, in comparison with substrates containing electron-poor aromatic substituents. The related N-allylic alkylation of 3-aminoquinazolinones **88** was also successful, and the atropselective synthesis of chiral quinazolinones **89** bearing an N–N bond was also achieved. Both the substituents on the benzene ring of the quinazolinones and the protective groups on the exo-nitrogen, from ester to acyl and benzoyl, could be varied, with the ees of the products obtained remaining high. Racemization and DFT experiments were performed to obtain rotational barriers. The highest was that of **87a**, at  $\Delta G^\ddagger = 32.3 \text{ kcal mol}^{-1}$ . After heating in mesitylene at  $135^\circ\text{C}$ , the ee dropped to nearly 40% (31.7 kcal/mol, DFT). DFT calculations suggest that the origins of enantioselectivity arise from hydrogen bonding interactions between the quinidine catalyst and the substrate.

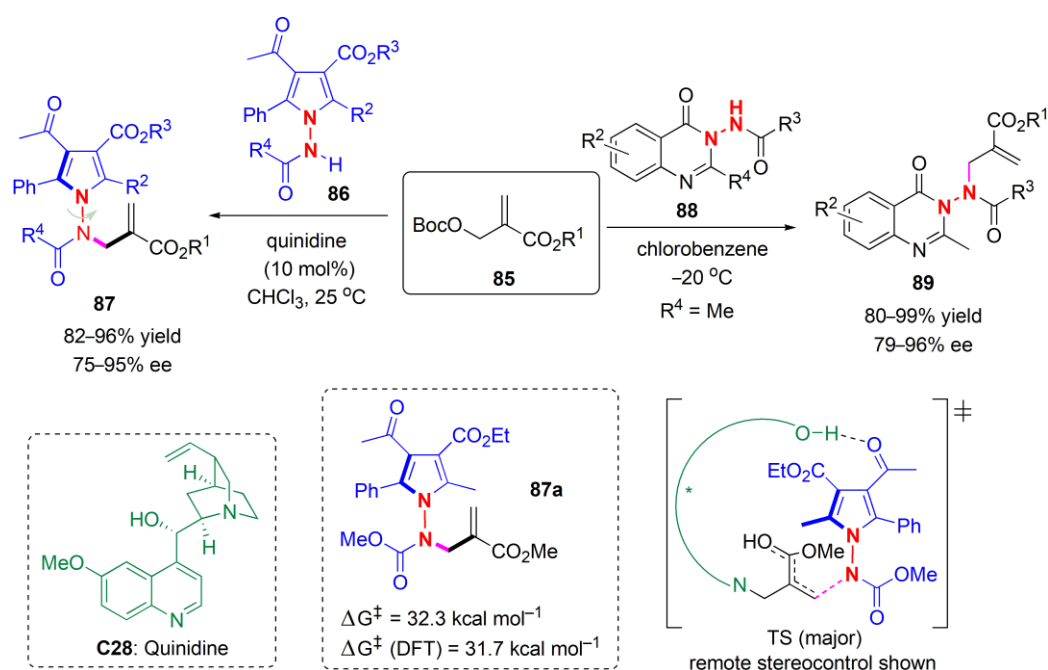


**Figure 27.** Atropselective synthesis of N–N axially chiral compounds **87** and **89** [32].

An interesting aspect that this research revealed was the fact that although the steric effect of the four *ortho*-substituents clearly played an essential role, the more distant functional groups at the C3- or C4-position of pyrrole ring had a significant effect on chirality transfer from catalyst to the prochiral N–N axis. When the C-3 acetyl group in **86** was replaced by H, the ee dropped to 36%, and when replaced by CN, it dropped to 4%, thereby confirming the existence of remote stereocontrol.

Soon after this report, Li and co-workers published a procedure to access N–N axially chiral quinazolinone derivatives via organocatalytic atropselective N-acylation of quinazolinon-type benzamides **88** with cinnamic anhydrides **90** (Figure 28) [70]. In products **91**, there are three rotation axes: the N–COR<sup>3</sup>, N–COCHCHAr, and N–N rotation axes. Very high yields, drs, and ees were obtained in the reactions for a large variety of substrates, with the simple chiral isothiourea **C29** as catalyst. The dr was >19:1 in all cases.

A large-scale reaction was also possible with no deterioration in the results. The products could also be used as acylation kinetic resolution reagents.

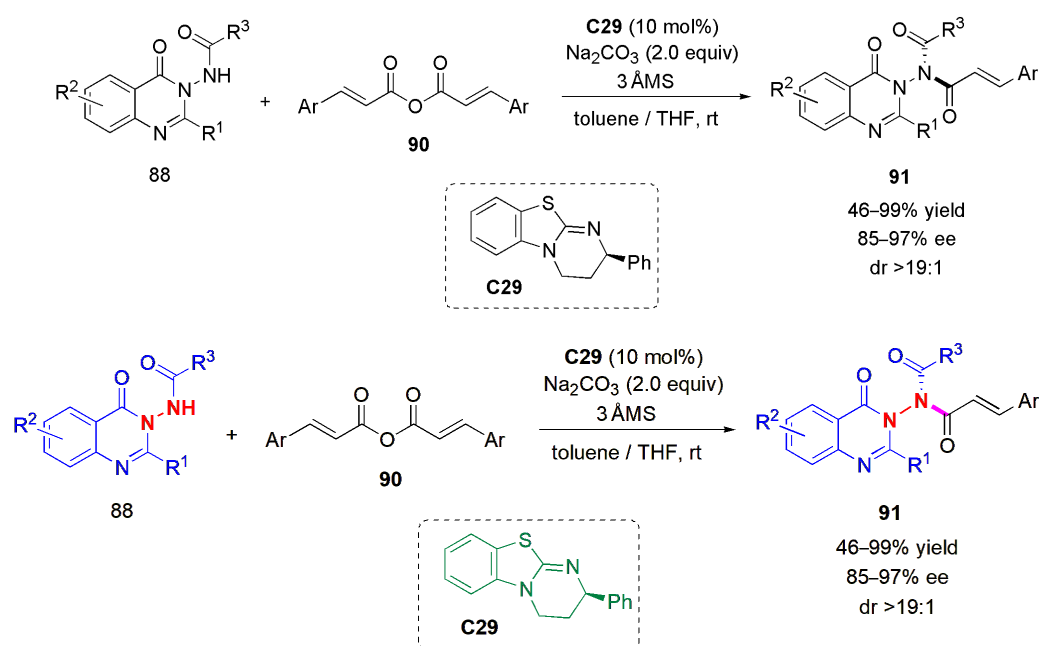


**Figure 28.** Asymmetric synthesis of N–N axially chiral compounds via organocatalytic atroposelective N-acylation [70].

The first highly atroposelective construction of N–N axially chiral indoles was reported in 2022 [71]. In this case, the strategy utilized by Zhang, Shi, and co-workers was de novo ring formation. An organocatalytic asymmetric Paal–Knorr reaction of 1,4-diketones **56** with *N*-aminoindoles **92** afforded *N*-pyrrolylindoles **93** in high yields, and with excellent atroposelectivities in the presence of **C30** (Figure 29). The same strategy could be applied to the atroposelective synthesis of N–N axially chiral bispyrroles **95** from compounds **94**. The stability of two selected examples **93a** and **95a** was examined via stirring at a high temperature of 110 °C in toluene for 12 h. They were both recovered in nearly quantitative yields, retaining their high ee values, which shows that these compounds have high chemical and configurational stability. The rotational barriers were calculated and found to be much higher than the energy barrier of 24 kcal mol<sup>−1</sup> required to isolate the two atropisomers [71]. Their stability was attributed to the presence of the bulky *ortho* groups, i.e., ester, (substituted)phenyl, and 2-naphthyl groups, around the stereogenic N–N axis.

More recently Liu, Teng, and co-workers described an enantioselective synthetic route from compounds **90** and **96** to N–N axially chiral 3,3′-bisquinazolinones **97** (Figure 30) [72]. In this first report of an atroposelective synthesis of these substances, a dual-ring formation strategy was used, which afforded the desired compounds with good chemical yields and ees. Chiral phosphoric acid **C12** was the catalyst that provided the best results. The configurational stability of the new substances was proven when it was found that they did not racemize, even after being heated to 150 °C for 12 h, in an experiment performed with **97a**. It was proposed that the reaction follows a domino mechanism in which there is initially dual CPA-catalyzed cyclization, in which two chiral centers are created, followed by oxidation, with central to axial chirality transfer. The related bisquinazolinone **98** is known to have antibacterial and antifungal properties [73].

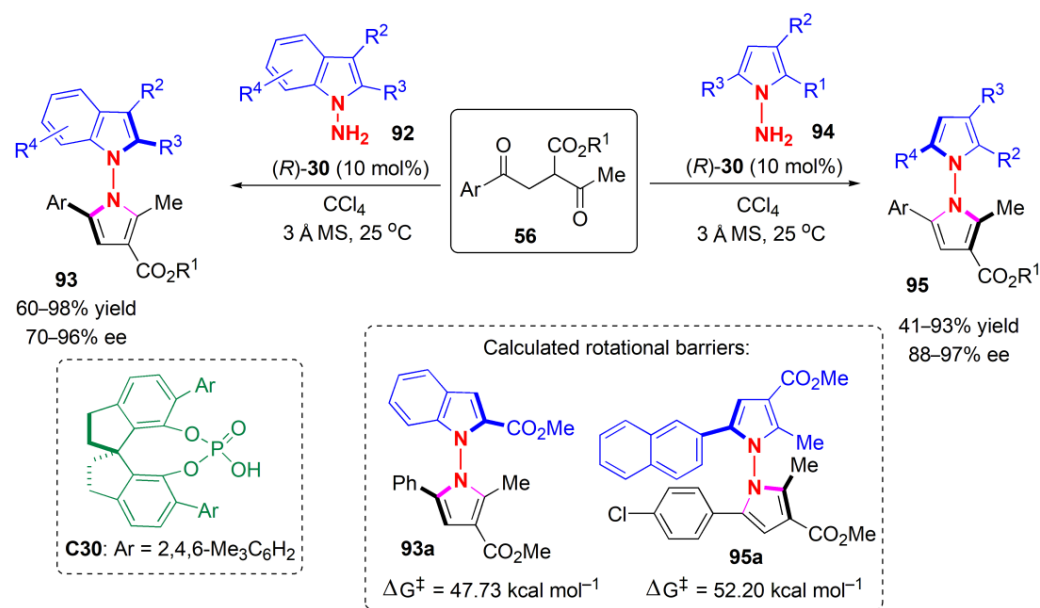


Figure 29. Atroposelective synthesis of N-N axially chiral indoles [71].

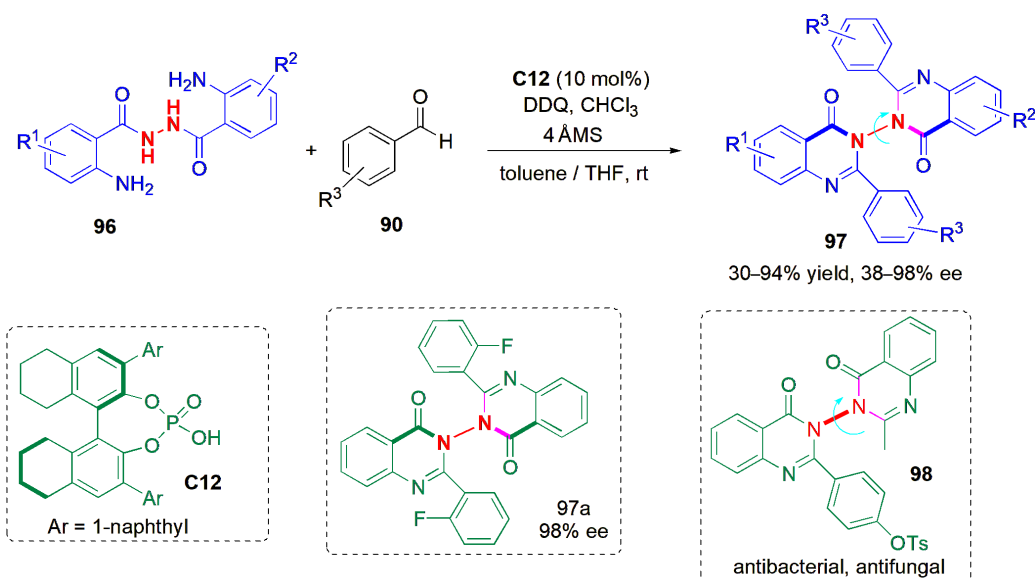


Figure 30. Atroposelective synthesis of N-N axially chiral 3,3'-bisquinazolinones [72].

#### 4. Conclusions

Stereoisomerism resulting from hindrance to rotation around a single bond in a molecule can give rise to compounds with different properties that can be isolated when the rotational energy barrier is large enough. However, if atropisomerism is present and it is undetected until a compound is used in its final application, unforeseen problems, including time-dependent racemization, may arise. This may be the case with pharmaceutical active ingredients, for example. Hence, the ability to synthesize atropisomers independently in order to study their properties, including the energy barrier to rotation, and to ascertain their stability is highly desirable, and has led to several developments in recent years. Atropisomers, and particularly C-N atropisomers, play important roles in medicinal chemistry, in natural product chemistry, in the production of functional materials such as OLEDs, and in the emerging area of molecular rotors. Axially chiral ligands, e.g., BINOL, BINAP, BINAM, and chiral phosphoric acid or quaternary amine organocatalysts, for example, have contributed significantly to the development of asymmetric catalysis. Traditionally atropisomers have been obtained mainly via recrystallization or resolution. Of

late, a large number of mild, sustainable organocatalytic procedures have been developed in order to obtain these substances in an enantioselective way. C-N atropisomers and N-N atropisomers may be synthesized in this manner, the latter since 2021. The approaches used include C-H amination, N-H functionalization, N-H amination, desymmetrization, and methods relying on the formation of one or more rings. In recent years, there has also been an evolution from biaryl to heterobiaryl to non-biaryl structures. Applications of the newer structures, such as ligands or organocatalysts, are still very limited, and this is a research area that will continue to expand. The synthesis of heterobiaryls is still in its infancy, and this is a field in which growth is also expected in the near future. This review provides an overview of recent achievements in the synthesis of atropisomers containing C-N and N-N axes of chirality, and the authors hope that the developments reported spark even greater interest in this fascinating subject area.

**Author Contributions:** A.M.F.P.: planning and writing; A.J.L.P.: advice and discussions. All authors have read and agreed to the published version of the manuscript.

**Funding:** This research received no external funding.

**Data Availability Statement:** There is no other data associated with this paper, since it is a review of the current literature.

**Acknowledgments:** Funding by Fundação para a Ciência e a Tecnologia (FCT), Portugal, in the form of projects UIDB/00100/2020 and UIDP/00100/2020 of Centro de Química Estrutural and project LA/P/0056/2020 of the Institute of Molecular Sciences is gratefully acknowledged. AMFP also thanks FCT for finance in the form of project EXPL/QUI-QOR/1079/2021. The work was also supported by the RUDN University Strategic Academic Leadership Program (recipient A.J.L.P.).

**Conflicts of Interest:** The authors declare no conflict of interest.

## References

1. IUPAC. Compendium of Chemical Terminology. In *The "Gold Book"*, 2nd ed.; McNaught, A.D., Wilkinson, A., Eds.; Blackwell Scientific Publications: Oxford, UK, 1997; ISBN 0-9678550-9-8. [[CrossRef](#)]
2. Carlsson, A.-C.C.; Karlsson, S.; Munday, R.H.; Tatton, M.R. Approaches to Synthesis and Isolation of Enantiomerically Pure Biologically Active Atropisomers. *Acc. Chem. Res.* **2022**, *55*, 2938–2948. [[CrossRef](#)] [[PubMed](#)]
3. Oki, M. Recent Advances in Atropisomerism. In *Topics in Stereochemistry*; Allinger, N.L., Eliel, N.L., Wilen, S.H., Eds.; John Wiley & Sons: New York, NY, USA, 1983; Volume 14, pp. 1–81.
4. LaPlante, S.R.; Edwards, P.J.; Fader, L.D.; Jakalian, A.; Hucke, O. Revealing Atropisomer Axial Chirality in Drug Discovery. *ChemMedChem* **2011**, *6*, 505–513. [[CrossRef](#)] [[PubMed](#)]
5. Sahoo, D.; Benny, R.; Kumar, N.; De, S. Stimuli-Responsive Chiroptical Switching. *ChemPlusChem* **2022**, *87*, e2021003. [[CrossRef](#)] [[PubMed](#)]
6. Dial, B.E.; Pellechia, P.J.; Smith, M.D.; Shimizu, K.D. Proton Grease: An Acid Accelerated Molecular Rotor. *J. Am. Chem. Soc.* **2012**, *134*, 3675–3678. [[CrossRef](#)]
7. Anirban Mondal, A.; Toyoda, R.; Costil, R.; Feringa, B.L. Chemically Driven Rotatory Molecular Machines. *Angew. Chem. Int. Ed.* **2022**, *61*, e202206631.
8. Xie, J.-H.; Zhou, Q.-L. Chiral Diphosphine and Monodentate Phosphorus Ligands on a Spiro Scaffold for Transition-Metal-Catalyzed Asymmetric Reactions. *Acc. Chem. Res.* **2008**, *41*, 581–593. [[CrossRef](#)]
9. da Silva, E.M.; Vidal, H.D.A.; Januário, M.A.P.; Corrêa, A.G. Advances in the Asymmetric Synthesis of BINOL Derivatives. *Molecules* **2023**, *28*, 12. [[CrossRef](#)]
10. Ding, K.; Li, X.; Ji, B.; Guo, H.; Kitamura, M. Ten Years of Research on NOBIN Chemistry Author(s). *Curr. Org. Synth.* **2005**, *2*, 499–545. [[CrossRef](#)]
11. Akiyama, T.; Mori, K. Stronger Brønsted Acids: Recent Progress. *Chem. Rev.* **2015**, *115*, 9277–9306. [[CrossRef](#)]
12. Cheng, J.K.; Xiang, S.-H.; Tan, B. Organocatalytic Enantioselective Synthesis of Axially Chiral Molecules: Development of Strategies and Skeletons. *Acc. Chem. Res.* **2022**, *55*, 2920–2937. [[CrossRef](#)]
13. LaPlante, S.R.; Fader, L.D.; Fandrick, K.R.; Fandrick, D.R.; Hucke, O.; Kemper, R.; Miller, S.P.F.; Edwards, P.J. Assessing Atropisomer Axial Chirality in Drug Discovery and Development. *J. Med. Chem.* **2011**, *54*, 7005–7022. [[CrossRef](#)] [[PubMed](#)]
14. Basilaia, M.; Chen, M.H.; Secka, J.; Gustafson, J.L. Atropisomerism in the Pharmaceutically Relevant Realm. *Acc. Chem. Res.* **2022**, *55*, 2904–2919. [[CrossRef](#)] [[PubMed](#)]
15. Perreault, S.; Chandrasekhar, J.; Patel, L. Atropisomerism in Drug Discovery: A Medicinal Chemistry Perspective Inspired by Atropisomeric Class I PI3K Inhibitors. *Acc. Chem. Res.* **2022**, *55*, 2581–2593. [[CrossRef](#)] [[PubMed](#)]

16. Zilate, B.; Castrogiovanni, A.; Sparr, C.S. Catalyst-Controlled Stereoselective Synthesis of Atropisomers. *ACS Catal.* **2018**, *8*, 2981–2988. [[CrossRef](#)]
17. Yang, Y.-D.; Yang, B.B.; Li, L. A Nonneglectable Stereochemical Factor in Drug Development: Atropisomerism. *Chirality* **2022**, *34*, 1355–1370. [[CrossRef](#)]
18. Wang, Z.; Meng, L.; Liu, X.; Zhang, L.; Yu, Z.; Wu, G. Recent Progress toward Developing Axial Chirality Bioactive Compounds. *Eur. J. Med. Chem.* **2022**, *243*, 114700. [[CrossRef](#)]
19. Bencivenni, G. Organocatalytic Strategies for the Synthesis of Axially Chiral Compounds. *Synlett* **2015**, *26*, 1915–1922. [[CrossRef](#)]
20. Wencel-Delord, J.; Panossian, A.; Leroux, F.R.; Colobert, F. Recent Advances and New Concepts for the Synthesis of Axially Stereoenriched Biaryls. *Chem. Soc. Rev.* **2015**, *44*, 3418–3430. [[CrossRef](#)]
21. Kumarasamy, E.; Raghunathan, R.; Sibi, M.P.; Sivaguru, J. Nonbiaryl and Heterobiaryl Atropisomers: Molecular Templates with Promise for Atroposelective Chemical Transformations. *Chem. Rev.* **2015**, *115*, 11239–11300. [[CrossRef](#)]
22. Wang, Y.-B.; Tan, B. Construction of Axially Chiral Compounds via Asymmetric Organocatalysis. *Acc. Chem. Res.* **2018**, *51*, 534–547. [[CrossRef](#)]
23. Woldegiorgis, A.G.; Lin, X. Recent Advances in the Asymmetric Phosphoric Acid-Catalyzed Synthesis of Axially Chiral Compounds. *Beilstein J. Org. Chem.* **2021**, *17*, 2729–2764. [[CrossRef](#)]
24. Carmona, J.A.; Rodríguez-Franco, C.; Fernández, R.; Hornillos, V.; Lassaletta, J.M. Atroposelective Transformation of Axially Chiral (Hetero)Biaryls. From desymmetrization to Modern Resolution Strategies. *Chem. Soc. Rev.* **2021**, *50*, 2968–2983. [[CrossRef](#)] [[PubMed](#)]
25. van Capelle, L.A.C.; Macdonald, J.M.; Hyland, C.J.T. Stereogenic and Conformational Properties of Medium-Ring Benzo-Fused N-Heterocycle Atropisomers. *Org. Biomol. Chem.* **2021**, *19*, 7098–7115. [[CrossRef](#)]
26. Bai, X.-F.; Cui, Y.-M.; Cao, J.; Xu, L.-W. Atropisomers with Axial and Point Chirality: Synthesis and Applications. *Acc. Chem. Res.* **2022**, *55*, 2545–2561. [[CrossRef](#)]
27. Cheng, J.K.; Xiang, S.H.; Li, S.; Ye, L.; Tan, B. Recent Advances in Catalytic Asymmetric Construction of Atropisomers. *Chem. Rev.* **2021**, *121*, 4805–4902. [[CrossRef](#)]
28. Rodríguez-Salamanca, P.; Fernández, R.; Hornillos, V.; Lassaletta, J.M. Asymmetric Synthesis of Axially Chiral C-N Atropisomers. *Chem. Eur. J.* **2022**, *28*, e202104442. [[CrossRef](#)]
29. Sweet, J.S.; Knipe, P.C. Catalytic Enantioselective Synthesis of C-N Atropisomeric Heterobiaryls. *Synthesis* **2022**, *54*, 2119–2132. [[CrossRef](#)]
30. Lakhdar, S. Construction of Axially Chiral Compounds via Catalytic Asymmetric Radical Reaction. *Green Synth. Catal.* **2022**, *3*, 212–218.
31. Zhang, H.-H.; Shi, F. Organocatalytic Atroposelective Synthesis of Indole Derivatives Bearing Axial Chirality: Strategies and Applications. *Acc. Chem. Res.* **2022**, *55*, 2562–2580. [[CrossRef](#)] [[PubMed](#)]
32. Mei, G.-J.; Wong, J.J.; Zheng, W.; Nangia, A.A.; Houk, K.N.; Lu, Y. Rational Design and Atroposelective Synthesis of N-N Axially Chiral Compounds. *Chem* **2021**, *7*, 2743–2757. [[CrossRef](#)]
33. Zhang, Q.; Mándi, A.; Li, S.; Chen, Y.; Zhang, W.; Tian, X.; Zhang, H.; Li, H.; Zhang, W.; Zhang, S.; et al. N-N-coupled Indolosesquiterpene Atropo-Diastereomers from a Marine-Derived Actinomycete. *Eur. J. Org. Chem.* **2012**, *2012*, 5256–5262. [[CrossRef](#)]
34. Brandes, S.; Bella, M.; Kjærsgaard, A.; Jørgensen, K.A. Chirally Aminated 2-Naphthols—Organocatalytic Synthesis of Non-Biaryl Atropisomers by Asymmetric Friedel–Crafts Amination. *Angew. Chem.* **2006**, *118*, 1165–1169. [[CrossRef](#)]
35. Clayden, J. Non-Biaryl Atropisomers: New Classes of Chiral Reagents, Auxiliaries, and Ligands? *Angew. Chem. Int. Ed.* **1997**, *36*, 949–951. [[CrossRef](#)]
36. Kitagawa, O.; Takahashi, M.; Yoshikawa, M.; Taguchi, T.J. Efficient Synthesis of Optically Active Atropisomeric Anilides through Catalytic Asymmetric N-Arylation Reaction. *Am. Chem. Soc.* **2005**, *127*, 3676–3677. [[CrossRef](#)]
37. Bai, H.-Y.; Tan, F.-X.; Liu, T.-Q.; Zhu, G.-D.; Tian, J.-M.; Ding, T.-M.; Chen, Z.-M.; Zhang, S.-Y. Highly Atroposelective Synthesis of Nonbiaryl Naphthalene-1,2-Diamine N-C Atropisomers Through Direct Enantioselective C-H Amination. *Nat. Commun.* **2019**, *10*, 3063. [[CrossRef](#)]
38. Wang, D.; Jiang, Q.; Yang, X. Atroposelective Synthesis of Configurationally Stable Nonbiaryl N-C Atropisomers Through Direct Asymmetric Aminations of 1,3-Benzenediamines. *Chem. Commun.* **2020**, *56*, 6201–6204. [[CrossRef](#)]
39. Xia, W.; An, Q.J.; Xiang, S.H.; Li, S.; Wang, Y.B.; Tan, B. Chiral Phosphoric Acid Catalyzed Atroposelective C-H Amination of Arenes. *Angew. Chem. Int. Ed.* **2020**, *59*, 6775–6779. [[CrossRef](#)]
40. Shirakawa, S.; Liu, K.; Maruoka, K. Catalytic Asymmetric Synthesis of Axially Chiral *o*-Iodoanilides by Phase-Transfer Catalyzed Alkylations. *J. Am. Chem. Soc.* **2012**, *134*, 916–919. [[CrossRef](#)]
41. Li, S.L.; Yang, C.; Wu, Q.; Zheng, H.L.; Li, X.; Cheng, J.P. Atroposelective Catalytic Asymmetric Allylic Alkylation Reaction for Axially Chiral Anilides with Achiral Morita–Baylis–Hillman Carbonates. *J. Am. Chem. Soc.* **2018**, *140*, 12836–12843. [[CrossRef](#)]
42. Yang, G.-H.; Zheng, H.; Li, X.; Cheng, J.-P. Asymmetric Synthesis of Axially Chiral Phosphamides via Atroposelective N-Allylic Alkylation. *ACS Catal.* **2020**, *10*, 2324–2333. [[CrossRef](#)]
43. Charton, M. Nature of the Ortho Effect. II. Composition of the Taft Steric Parameters. *J. Am. Chem. Soc.* **1969**, *91*, 615–618. [[CrossRef](#)]

44. Diener, M.E.; Metrano, A.J.; Kusano, S.; and Miller, S.J. Enantioselective Synthesis of 3-Arylquinazolin-4(3*H*)-ones Via Peptide-Catalyzed Atroposelective Bromination. *J. Am. Chem. Soc.* **2015**, *137*, 12369–12377. [[CrossRef](#)]
45. Vaidya, S.D.; Toenjes, S.T.; Yamamoto, N.; Maddox, S.M.; Gustafson, J.L. Catalytic Atroposelective Synthesis of *N*-Aryl Quinoid Compounds. *J. Am. Chem. Soc.* **2020**, *142*, 2198–2203. [[CrossRef](#)]
46. Zhu, D.; Yu, L.; Luo, H.Y.; Xue, X.S.; Chen, Z.M. Atroposelective Electrophilic Sulfenylation of *N*-Aryl Aminoquinone Derivatives Catalyzed by Chiral SPINOL-Derived Sulfide. *Angew. Chem. Int. Ed.* **2022**, *61*, e202211782. [[CrossRef](#)] [[PubMed](#)]
47. Di Iorio, N.; Righi, P.; Mazzanti, A.; Mancinelli, M.; Ciogli, A.; Bencivenni, G. Remote Control of Axial Chirality: Aminocatalytic Desymmetrization of *N*-Arylmaleimides via Vinylogous Michael Addition. *J. Am. Chem. Soc.* **2014**, *136*, 10250–10253. [[CrossRef](#)]
48. Eudier, F.; Righi, P.; Mazzanti, A.; Ciogli, A.; Bencivenni, G. Organocatalytic Atroposelective Formal Diels-Alder Desymmetrization of *N*-Arylmaleimides. *Org. Lett.* **2015**, *17*, 1728–1731. [[CrossRef](#)]
49. Mondal, S.; Mukherjee, S. Catalytic Generation of Remote C–N Axial Chirality through Atroposelective *de novo* Arene Construction. *Org. Lett.* **2022**, *24*, 8300–8304. [[CrossRef](#)] [[PubMed](#)]
50. Barik, S.; Shee, S.; Das, S.; Gonnade, R.G.; Jindal, G.; Mukherjee, S.; Biju, A.T. NHC-Catalyzed Desymmetrization of *N*-Aryl Maleimides Leading to the Atroposelective Synthesis of *N*-Aryl Succinimides. *Angew. Chem. Int. Ed.* **2021**, *60*, 12264–12268. [[CrossRef](#)]
51. Zhang, J.W.; Xu, J.H.; Cheng, D.J.; Shi, C.; Liu, X.Y.; Tan, B. Discovery and Enantiocontrol Of Axially Chiral Urazoles via Organocatalytic Tyrosine Click Reaction. *Nat. Commun.* **2016**, *7*, 10677. [[CrossRef](#)]
52. Zhang, L.; Xiang, S.H.; Wang, J.J.; Xiao, J.; Wang, J.Q.; Tan, B. Phosphoric Acid-Catalyzed Atroposelective Construction of Axially Chiral Arylpyrroles. *Nat. Commun.* **2019**, *10*, 566. [[CrossRef](#)] [[PubMed](#)]
53. Bringmann, G.; Tasler, S.; Endress, H.; Kraus, J.; Messer, K.; Wohlfarth, M.; Lobin, W. Murrastifoline-F: First Total Synthesis, Atropo-Enantiomer Resolution, and Stereoanalysis of an Axially Chiral N,C-Coupled Biaryl Alkaloid. *J. Am. Chem. Soc.* **2011**, *123*, 2703–2711. [[CrossRef](#)] [[PubMed](#)]
54. Hughes, C.C.; Prieto-Davo, A.; Jensen, P.R.; Fenical, W. The Marinopyrroles, Antibiotics of an Unprecedented Structure Class from a Marine *Streptomyces* sp. *Org. Lett.* **2008**, *10*, 629–631. [[CrossRef](#)] [[PubMed](#)]
55. Zhang, L.; Zhang, J.; Ma, J.; Cheng, D.J.; Tan, B. Highly atroposelective synthesis of arylpyrroles by catalytic asymmetric Paal-Knorr reaction. *J. Am. Chem. Soc.* **2017**, *139*, 1714–1717. [[CrossRef](#)]
56. Min, C.; Lin, Y.; Seidel, D. Catalytic Enantioselective Synthesis of Mariline A and Related Isoindolinones through a Biomimetic Approach. *Angew. Chem. Int. Ed.* **2017**, *56*, 15353–15357. [[CrossRef](#)] [[PubMed](#)]
57. Wang, L.; Zhong, J.; Lin, X. Atroposelective Phosphoric Acid Catalyzed Three-Component Cascade Reaction: Enantioselective Synthesis of Axially Chiral *N*-Arylindoles. *Angew. Chem. Int. Ed.* **2019**, *58*, 15824–15828. [[CrossRef](#)]
58. Sha, Q.; Arman, H.; Doyle, M.P. Three-Component Cascade Reactions with 2,3-Diketooesters: A Novel Metal-Free Synthesis of 5-Vinyl-pyrrole and 4-Hydroxy-indole Derivatives. *Org. Lett.* **2015**, *17*, 3876. [[CrossRef](#)]
59. Wang, Y.B.; Zheng, S.C.; Hu, Y.M.; Tan, B. Bronsted Acid-Catalysed Enantioselective Construction of Axially Chiral Arylquinazolinones. *Nat. Commun.* **2017**, *8*, 15489.
60. Li, T.; Mou, C.; Qi, P.; Peng, X.; Jiang, S.; Hao, G.; Xue, W.; Yang, S.; Hao, L.; Chi, Y.R.; et al. *N*-Heterocyclic Carbene-Catalyzed Atroposelective Annulation for Access to Thiazine Derivatives with C–N Axial Chirality. *Angew. Chem. Int. Ed.* **2021**, *60*, 9362–9367. [[CrossRef](#)]
61. Rai, A.; Singh, A.K.; Raj, V.; Saha, S. 1,4-Benzothiazines-A Biologically Attractive Scaffold. *Mini-Rev. Med. Chem.* **2018**, *18*, 42. [[CrossRef](#)]
62. DePestel, D.D.; Benninger, M.S.; Danziger, L.; LaPlante, K.L.; May, C.; Luskin, A.; Pichichero, M.; Hadley, J.A. Cephalosporin Use in Treatment of Patients with Penicillin Allergies. *J. Am. Pharm. Assoc.* **2008**, *48*, 530–540. [[CrossRef](#)]
63. Chen, Y.; Li, T.; Jin, Z.; Chi, Y.R. New Axially Chiral Molecular Scaffolds with Antibacterial Activities against *Xanthomonas oryzae* pv. *oryzae* for Protection of Rice. *J. Agric. Food Chem.* **2022**, *70*, 6050–6058. [[CrossRef](#)]
64. Sanya, D.R.A.; Syed-Ab-Rahman, S.F.; Jia, A.; Onésime, D.; Kim, K.M.; Ahohuendo, B.C.; Rohr, J.R. Review of Approaches to Control Bacterial Leaf Blight in Rice. *World J. Microbiol. Biotechnol.* **2022**, *38*, 113. [[CrossRef](#)]
65. An, Q.J.; Xia, W.; Ding, W.Y.; Liu, H.H.; Xiang, S.H.; Wang, Y.B.; Zhong, G.; Tan, B. Nitrosobenzene-Enabled Chiral Phosphoric Acid Catalyzed Enantioselective Construction of Atropisomeric *N*-Arylbenzimidazoles. *Angew. Chem. Int. Ed.* **2021**, *60*, 24888–24893. [[CrossRef](#)]
66. Kim, A.; Kim, A.; Park, S.; Kim, S.; Jo, H.; Ok, K.M.; Lee, S.K.; Song, J.; Kwon, Y. Catalytic and Enantioselective Control of the C–N Stereogenic Axis via the Pictet–Spengler Reaction. *Angew. Chem. Int. Ed.* **2021**, *60*, 12279–12283. [[CrossRef](#)]
67. Seayad, J.; Seayad, A.M.; List, B. Catalytic Asymmetric Pictet–Spengler Reaction. *J. Am. Chem. Soc.* **2006**, *128*, 1086–1087. [[CrossRef](#)] [[PubMed](#)]
68. Dalpozzo, R. The Chiral Pool in the Pictet–Spengler Reaction for the Synthesis of  $\beta$ -Carbolines. *Molecules* **2016**, *21*, 699. [[CrossRef](#)] [[PubMed](#)]
69. Barik, S.; Das, R.C.; Balanna, K.; Biju, A.T. Kinetic Resolution Approach to the Synthesis of C–N Axially Chiral *N*-Aryl Aminomaleimides via NHC-Catalyzed [3 + 3] Annulation. *Org. Lett.* **2022**, *24*, 5456–5461. [[CrossRef](#)]
70. Lin, W.; Zhao, Q.; Li, Y.; Pan, M.; Yang, C.; Yang, G.H.; Li, X. Asymmetric Synthesis of N–N Axially Chiral Compounds via Organocatalytic Atroposelective *N*-Acylation. *Chem. Sci.* **2022**, *13*, 141–148. [[CrossRef](#)]

71. Chen, K.W.; Chen, Z.H.; Yang, S.; Wu, S.F.; Zhang, Y.C.; Shi, F. Organocatalytic Atroposelective Synthesis of N–N Axially Chiral Indoles and Pyrroles by De Novo Ring Formation. *Angew. Chem. Int. Ed.* **2022**, *61*, e202116829.
72. Pu, L.-Y.; Zhang, Y.-J.; Liu, W.; Teng, F. Chiral Phosphoric Acid-Catalyzed Dual-Ring Formation for Enantioselective Construction of N–N Axially Chiral 3,30-Bisquinazolinones. *Chem. Commun.* **2022**, *58*, 13131–13134. [[CrossRef](#)]
73. Reddy, P.S.; Bhavani, A.K.D. *N,N'*-Bisazaheterocycles: Synthesis and Importance. *Adv. Heterocycl. Chem.* **2015**, *114*, 271–391.

**Disclaimer/Publisher's Note:** The statements, opinions and data contained in all publications are solely those of the individual author(s) and contributor(s) and not of MDPI and/or the editor(s). MDPI and/or the editor(s) disclaim responsibility for any injury to people or property resulting from any ideas, methods, instructions or products referred to in the content.